Assessing the precision and accuracy of cavity ring-down spectroscopy measurements

Joseph T. Hodges

Material Measurement Laboratory,
National Institute of Standards and Technology,
Gaithersburg, MD

joseph.hodges@nist.gov

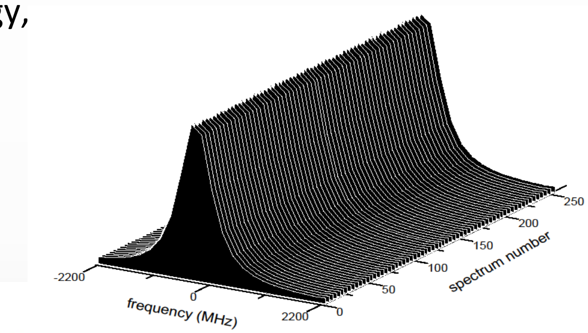

250 spectra in 0.7 s

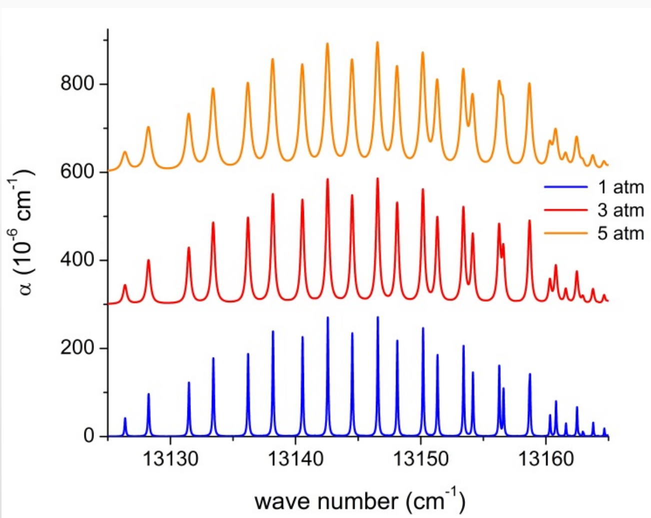

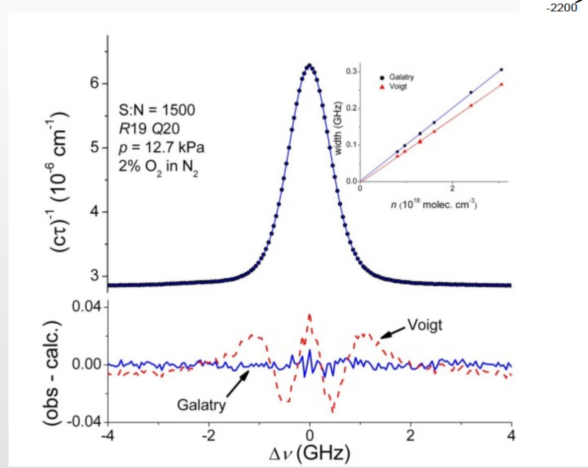

11th Annual International User Meeting
and Summer School on Cavity-Enhanced Spec
June 16-19, 2015, Boulder CO

National Institute of Standards and Technology • U.S. Department of Commerce

Factors affecting the precision of cw-CRDS measurements

Quantum fluctuations in photocurrent (shot noise)

Detector noise & signal digitization

Spurious coupling into high-order transverse modes

Finite beam extinction ratio

Drift and fluctuations in base cavity losses from:
- mirror birefringence & polarization-dependent losses
- coupled-cavity effects (etalons)
- spatially non-uniform losses & gas adsorption at mirrors

Factors affecting the accuracy of cw-CRDS measurements

Poorly constrained spectrum frequency detuning axis

Residual mode beating and improperly weighted fits

Detector/digitizer non-linearity and limited bandwidth

Saturation effects

Overly simplistic line shape models (e.g. Voigt Profile)

Experimental artifacts in spectrum baselines (etalons, birefringence etc.)

Sample characterization (temperature, pressure, molar fraction, wall effec

Properties of high-finesse resonators

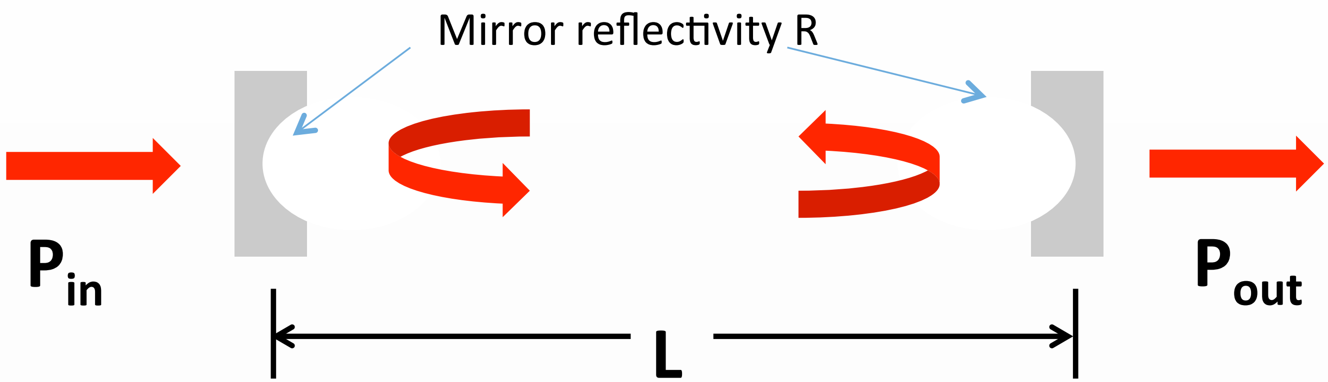

nces occur at multiples of c/2L — **comb-like structure, may provide spectrum "ruler"**

2L)/($\Delta\nu_{mode}$)= π/(1 – R) — **cavity finesse**

nce width is $\Delta\nu_{mode}$ = (c/2L)/F — **exceptionally good frequency filter, [typically ~1 to 50**

ve interaction path length is L_{eff} = (F/π)*L — **yields high-sensitivity to light absorption by cavity m**

interrogated via cw transmission or by observing passive decays (ring-down)

A little history …
multi-mode CRDS signal (pulsed excitation)

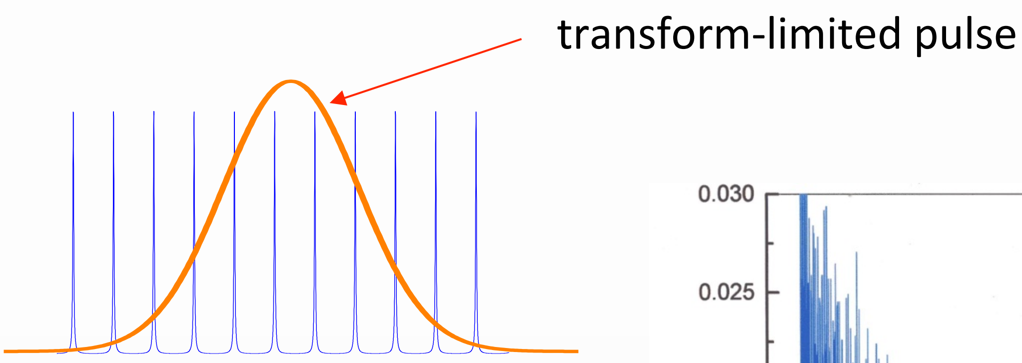

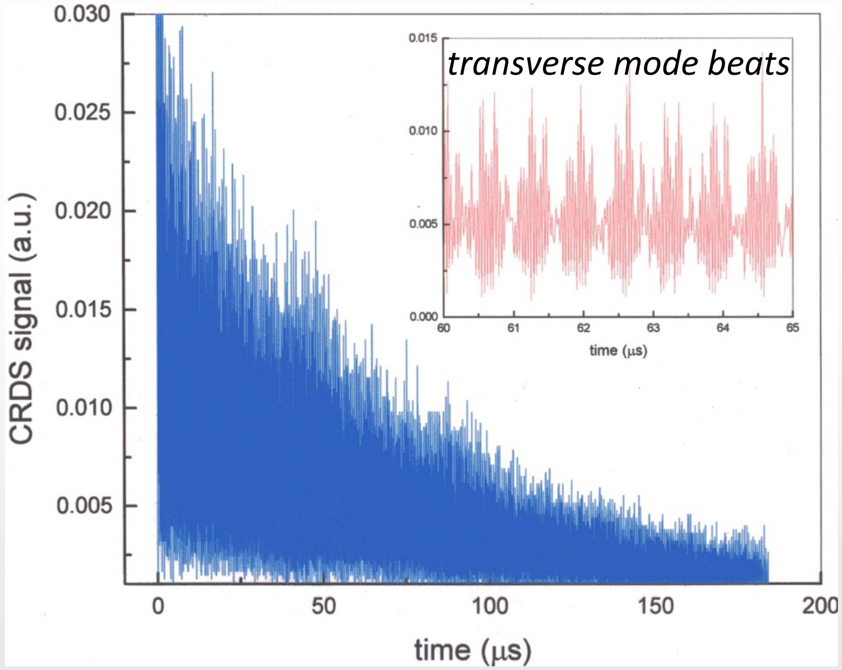

Signals were dominated by transverse and longitudinal mode beating effects, resulting in suboptimal statistics and severely compromised frequency resolution.

Single-mode cavity ring-down spectroscopy

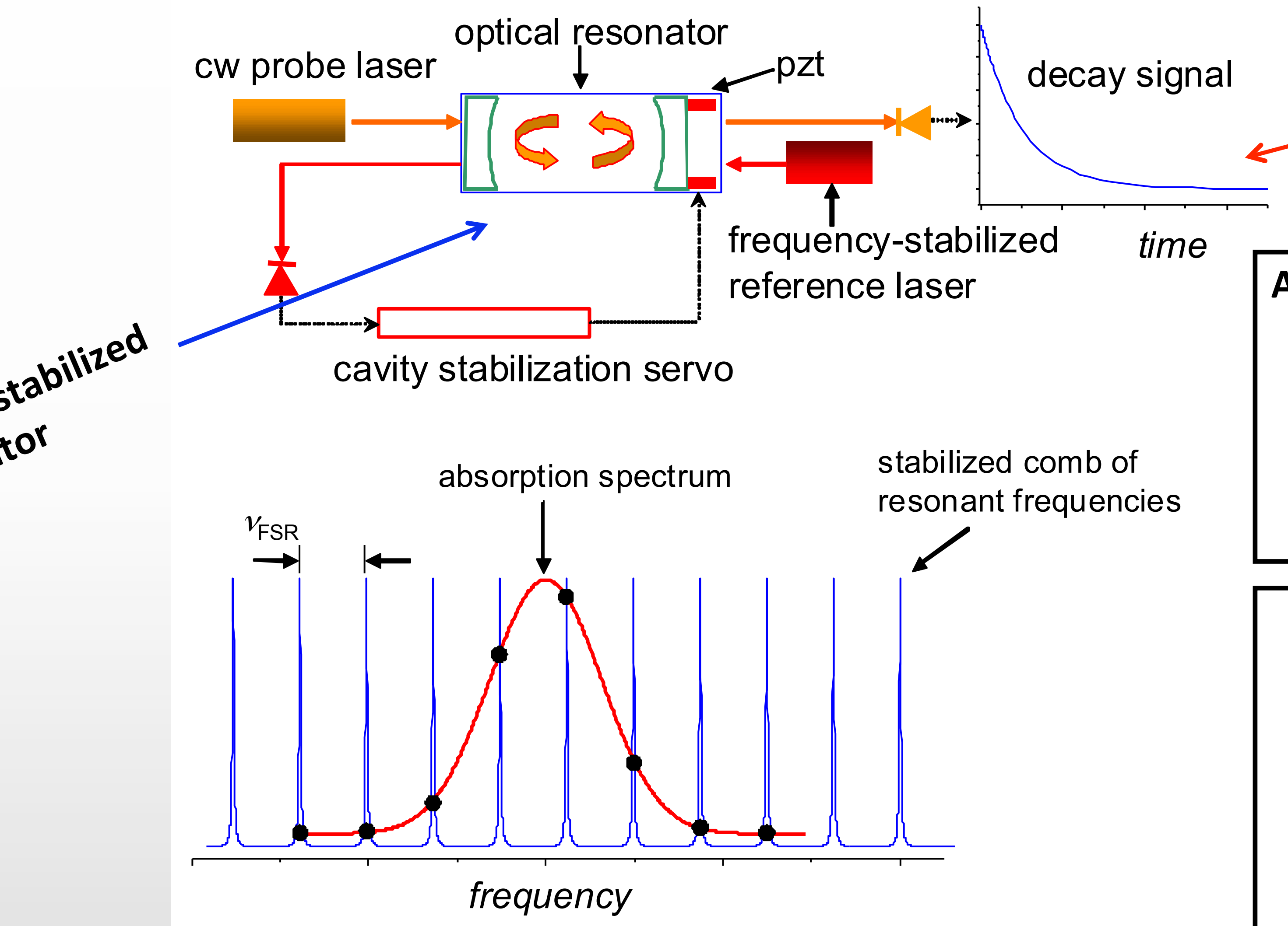

$S(t) = S_0 \exp\text{-}(t/\tau)$

Alternative length stabilization m

Ring-down cavity locked to probe
which is locked to a stabilized
external resonator

Temperature-controlled system

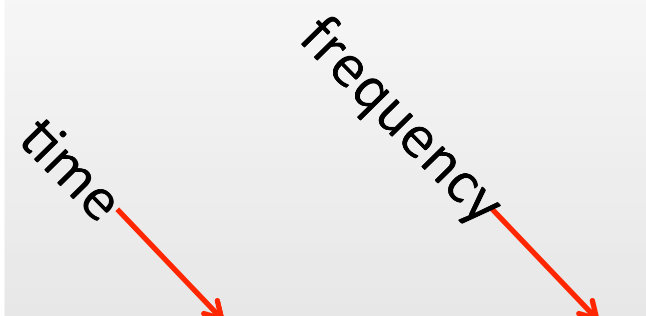

$1/(c\,\tau) = \alpha_0 + \alpha(\nu$

With length-stabilization, single-mode excitation enables high-fidelity and high-sensitivity measurements of transition areas, widths & shapes, positions and pressure shifts

Spectral scans (mode jumping)

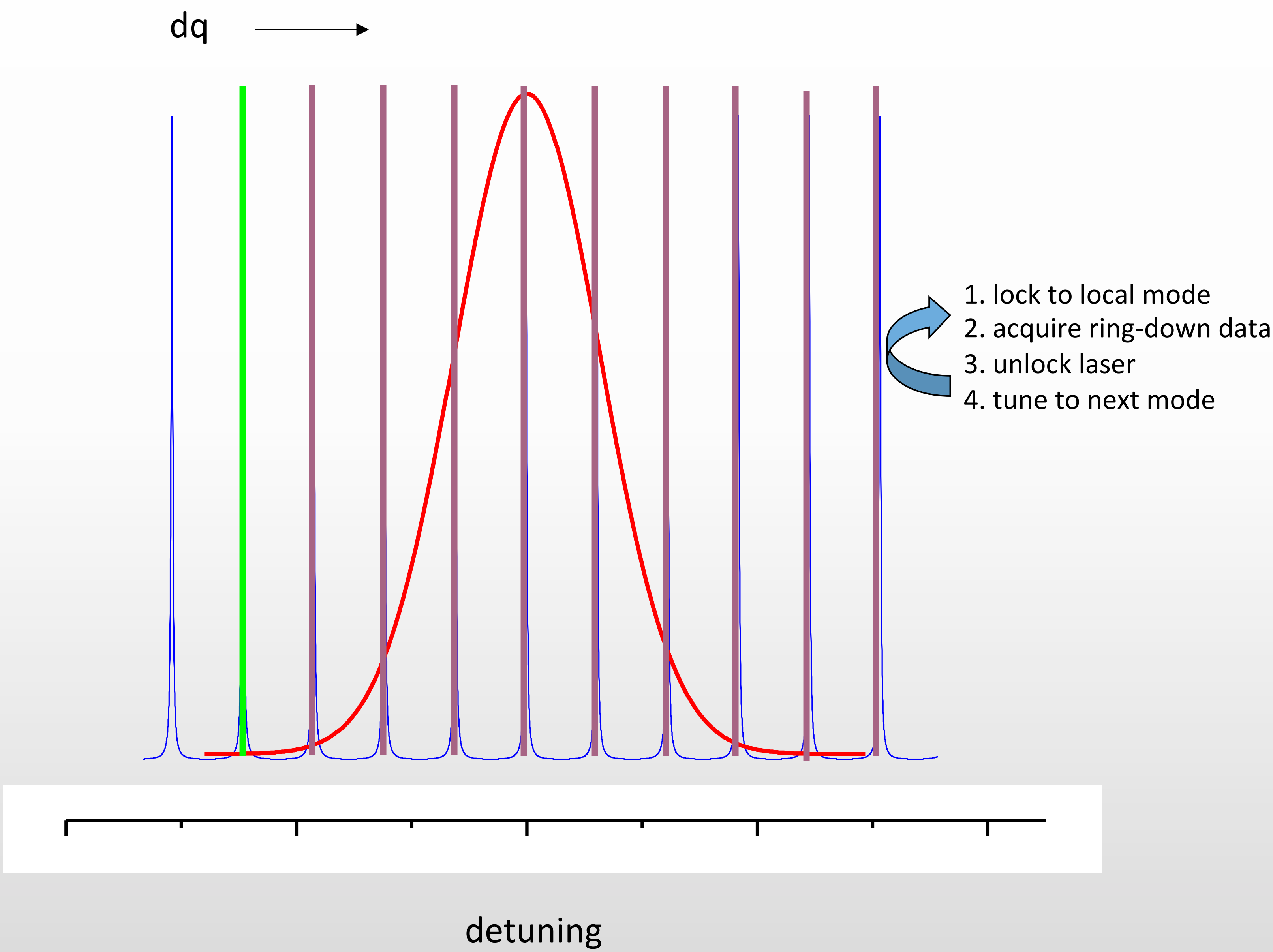

Spectral scans (shifting of frequency comb)

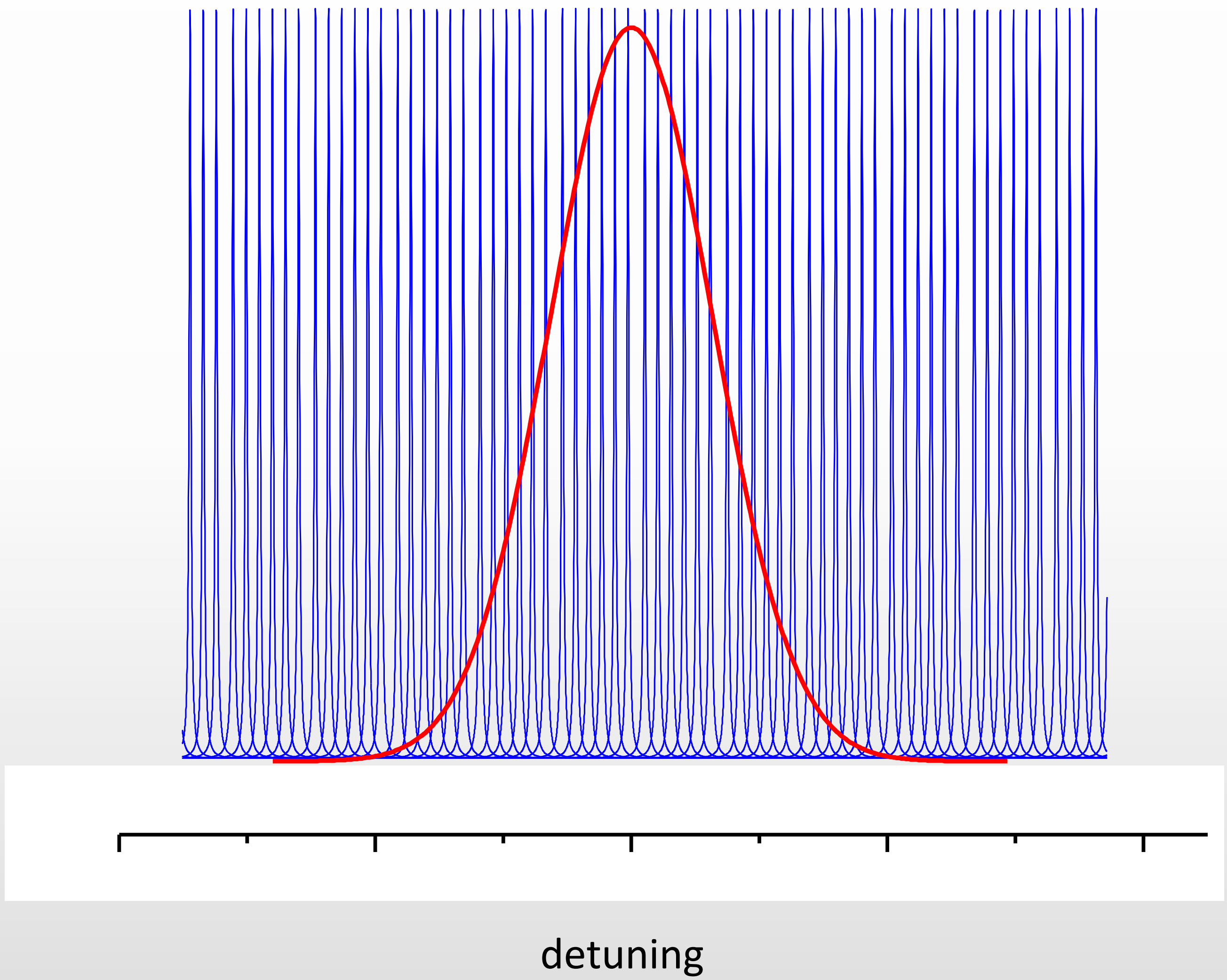

1. lock to local r
2. acquire ring-d
3. shift comb wi
4. laser tracks c

Noise-Equivalent Absorption Coefficient (NEA)

responds to the standard error in the cavity losses a 1 s averaging time (units: cm^{-1}/Hz$^{1/2}$)

$$_{in} = \frac{\sigma_\tau}{\tau}\frac{L_{mirr}}{\ell}\frac{1}{\sqrt{N_{dec}}} = \frac{\sigma_\tau}{\tau}\frac{L_{mirr}}{\ell}\frac{1}{\sqrt{f_{acq}\Delta t_{av}}}$$

$$\mathrm{NEA} = \alpha_{min}\sqrt{\Delta t_{av}} = \frac{\sigma_\tau}{\tau}\frac{L_{mirr}}{\ell}\frac{1}{\sqrt{f_{acq}}}$$

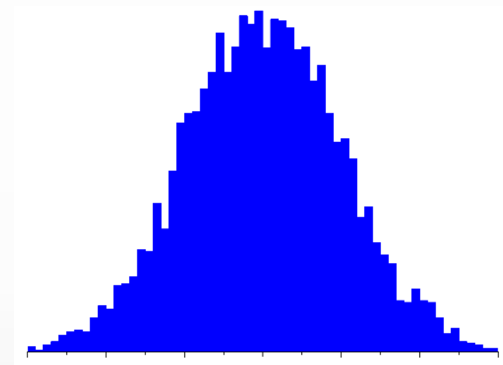

Distribution of measured time constants with mea value, τ and standard deviation, σ_τ.

Allan Variance

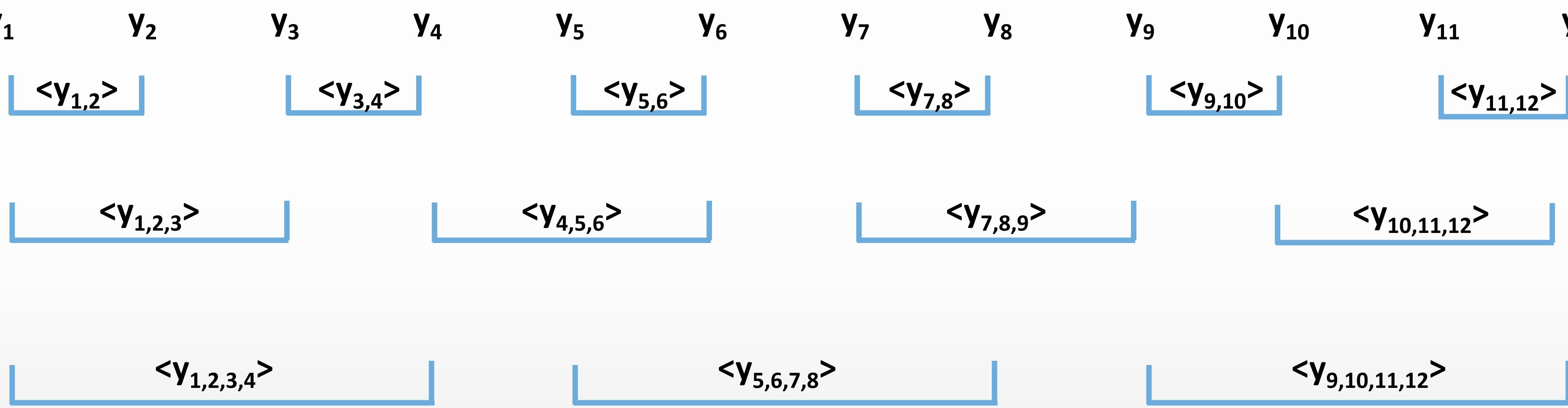

n upper bound on the time scale over which the measurements are statistically stationary

o specify the noise-equivalent absorption coefficient in (cm^{-1} Hz$^{-1/2}$) and minimum detectable ab

Allan Deviation Plot

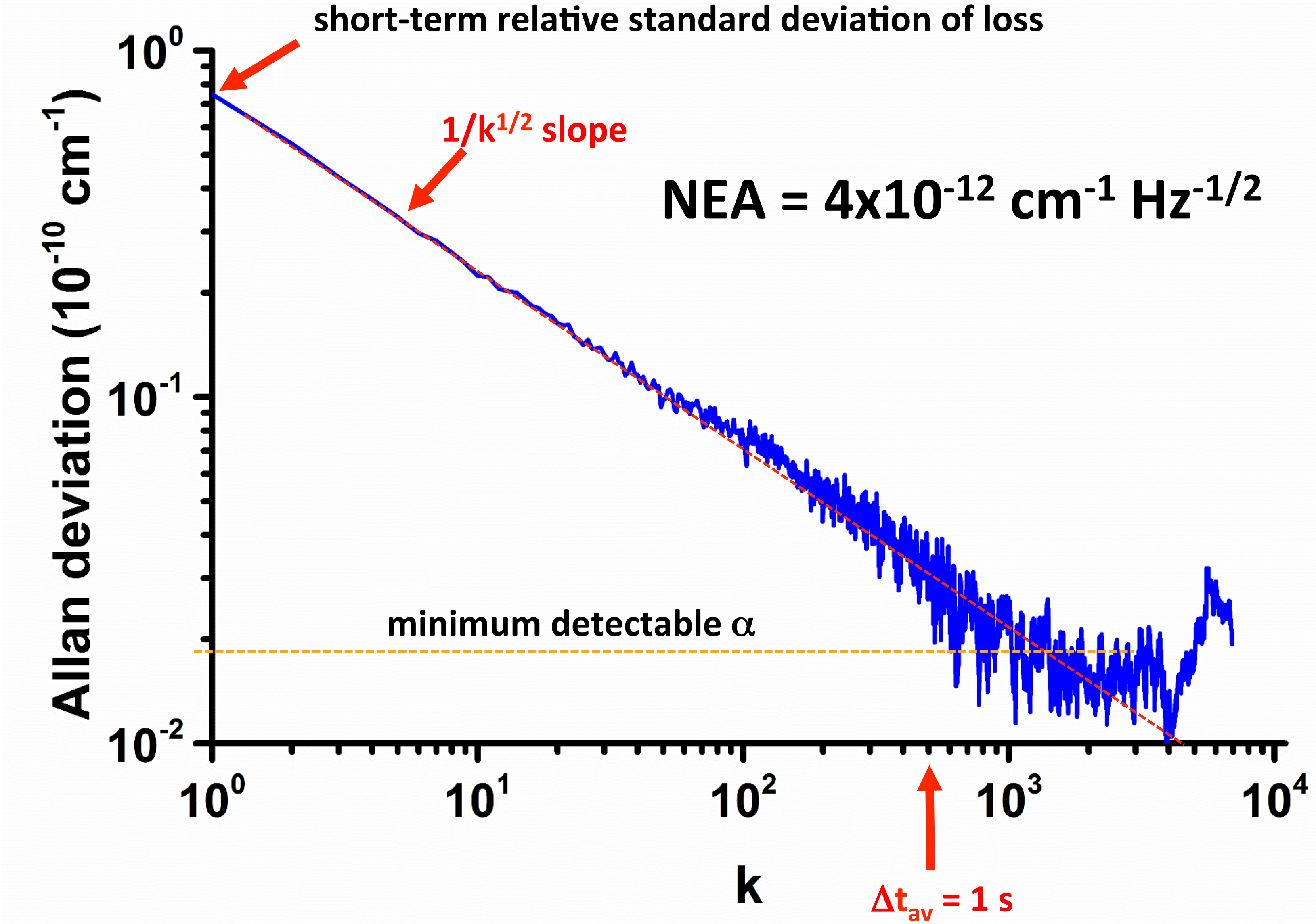

f_{acq} = 500

Shot Noise for CW signals

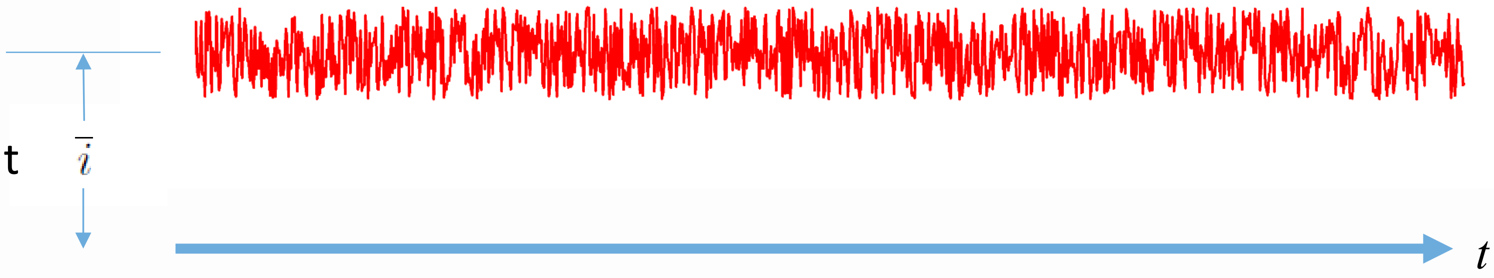

$$\sigma_{tech} = \sqrt{2e\bar{i}\Delta f}$$

$$SNR = \frac{\bar{i}}{\sigma_{tech}} = \sqrt{\frac{\bar{i}^2}{2e\bar{i}\Delta f}} = \sqrt{\frac{\bar{i}\Delta t_s}{e}} = \sqrt{N_e}$$

e signal-to-noise ratio corresponds to the square root of the
mber of photo-electrons, N_e in the sampling time interval, Δ

Noise limits for CRDS signals

Shot noise

RMS of noise decays exponentially with time constant of $\tau/2$

Integrating over decay gives $i_o\tau$ photoelectrons, N_e.

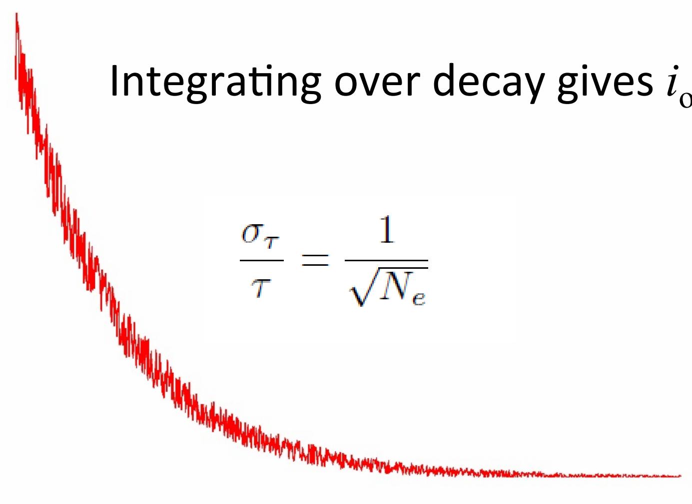

$$\frac{\sigma_\tau}{\tau} = \frac{1}{\sqrt{N_e}}$$

t

st be weighted to avoid bias in fitted τ

Technical noise

Noise has constant rms

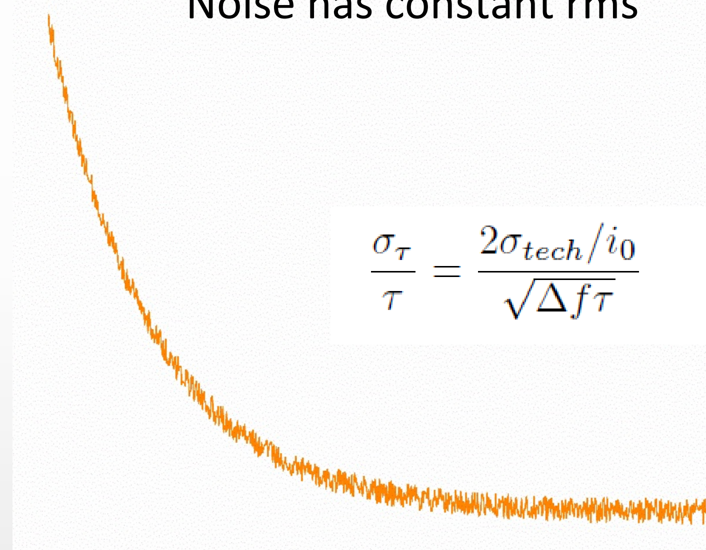

$$\frac{\sigma_\tau}{\tau} = \frac{2\sigma_{tech}/i_0}{\sqrt{\Delta f \tau}}$$

No weighting required

fect of birefringence and polarization-dependent loss

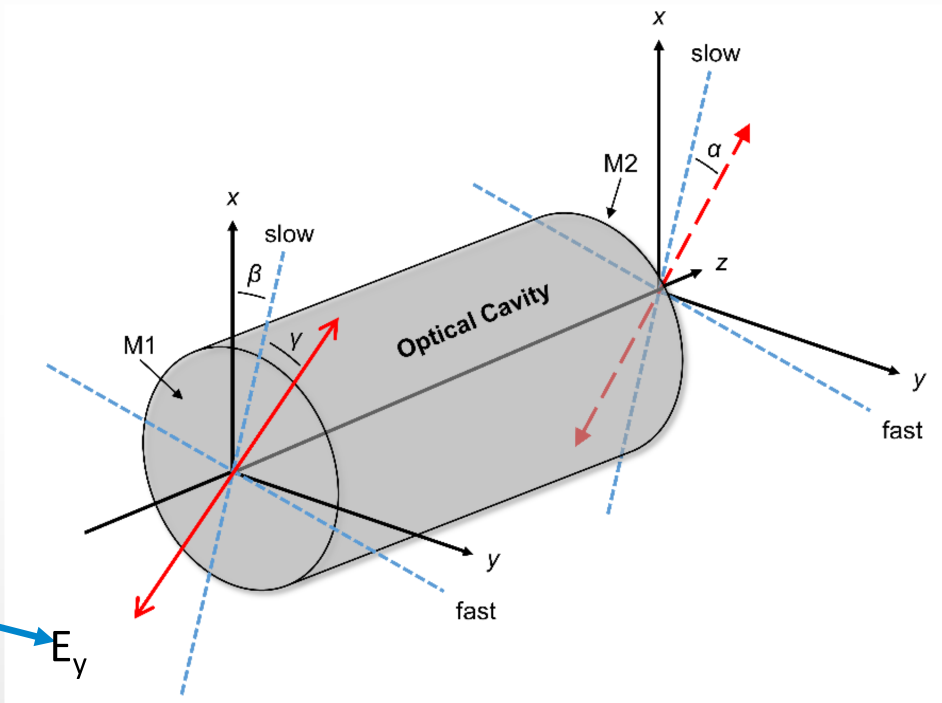

E$_y$

Can define effective “slow” and “fast” axes for the c

Difference in round-trip time for the two orthogona leads to slightly different resonant frequencies for t TEM_{00}

$\Delta\nu$~Δn*cavity free spectral range

Causes non-exponential decays & statistical broade of measured time constant

g & Lehmann, “Effects of linear birefringence and polarization-dependent loss of supermirrors in cavity ring-down spectro . Opt. **47**, 3817 (2008)

Birefringence and polarization-dependent losses

input: circularly polarized
with analyzer after cavity

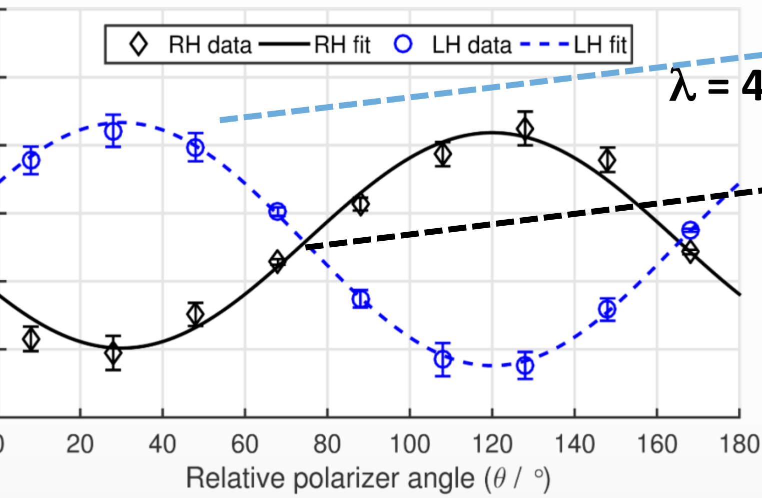

Residuals of fit to single exponential

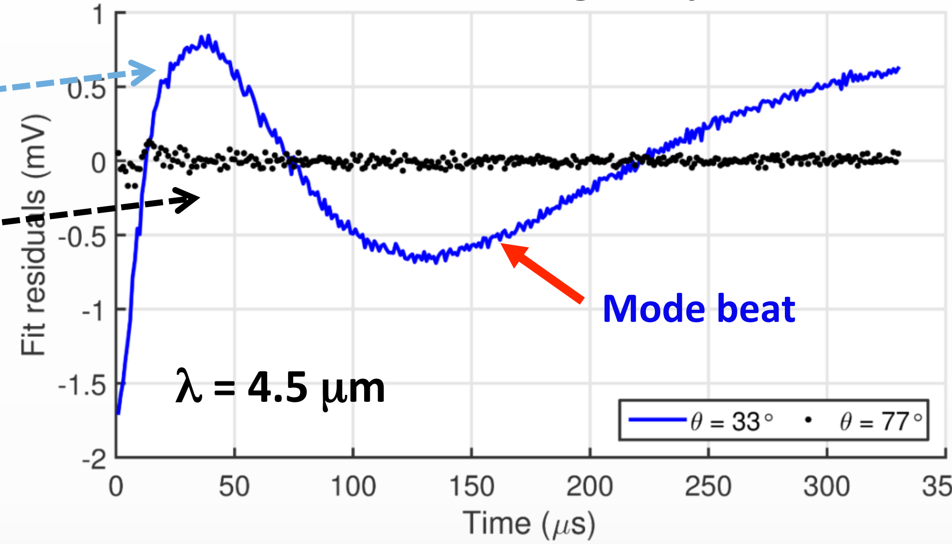

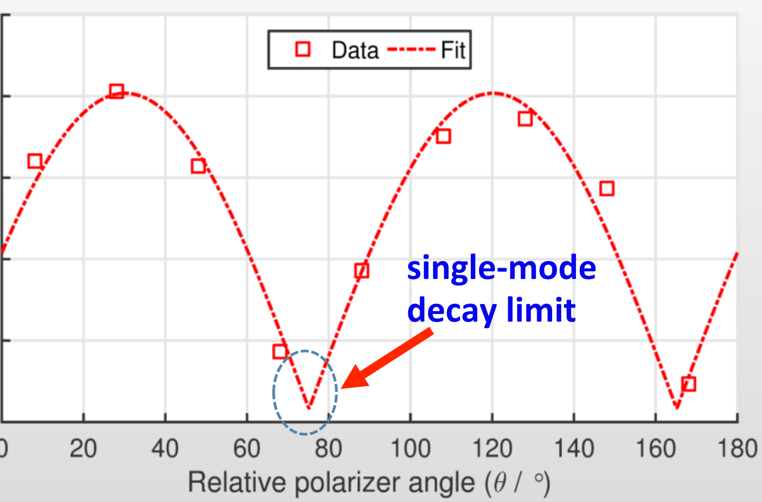

λ = 1.59 μm

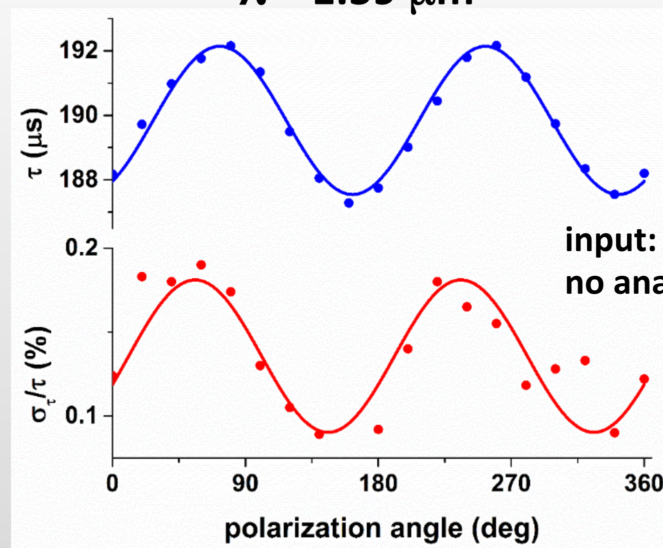

input: linearly polari
no analyzer after cav

High Order Transverse Modes

$$\nu_{qmn} = \frac{c}{2\ell}[\mathrm{q} + \frac{2}{\pi}\tan^{-1}(\frac{\ell}{\sqrt{\ell(2\mathrm{r} - \ell)}})(\mathrm{m} + \mathrm{n} + 1)]$$

ℓ = 157 cm, r = 100 cm

	Δq (MHz)	-12	-11	-10	-9	-8	-7	-6	-5	-4	-3	-2	-1	
Δmn (MHz)		Transverse Mode Beat Frequency (MHz)												
0		-1146	-1050	-955	-859	-764	-668	-573	-477	-382	-286	-191	-95	
1		-1080	-984	-889	-793	-698	-602	-507	-411	-316	-220	-125	-29	6
2		-1013	-918	-822	-727	-631	-536	-441	-345	-250	-154	-59	37	13
3		-947	-852	-756	-661	-565	-470	-374	-279	-183	-88	8	103	19
4		-881	-786	-690	-595	-499	-404	-308	-213	-117	-22	74	169	26
5		-815	-719	-624	-528	-433	-337	-242	-147	-51	44	140	235	33
6		-749	-653	-558	-462	-367	-271	-176	-80	15	111	206	302	39
7		-683	-587	-492	-396	-301	-205	-110	-14	81	177	272	368	46
8		-616	-521	-425	-330	-234	-139	-43	52	147	243	338	434	52
9		-550	-455	-359	-264	-168	-73	23	118	214	309	405	500	59
10		-484	-389	-293	-198	-102	-7	89	184	280	375	471	566	66
11		-418	-322	-227	-131	-36	60	155	250	346	441	537	632	72
12		-352	-256	-161	-65	30	126	221	317	412	508	603	699	79
13		-286	-190	-95	0.93	96	192	287	383	478	574	669	765	86
14		-219	-124	-28	67	163	258	354	449	544	640	735	831	92

$TEM_{6,7}$

Saturation in CRDS

nhomogeneously broadened case

$$G(t) = G_0 e^{-t/\tau_c} f(t; G_0, \tau_c, \tau_{abs})$$

$$dt = \frac{-2f(t)/\tau_{abs}}{1+\sqrt{1+G_0 e^{-t/\tau_c} f(t)}}, f(0) = 1$$

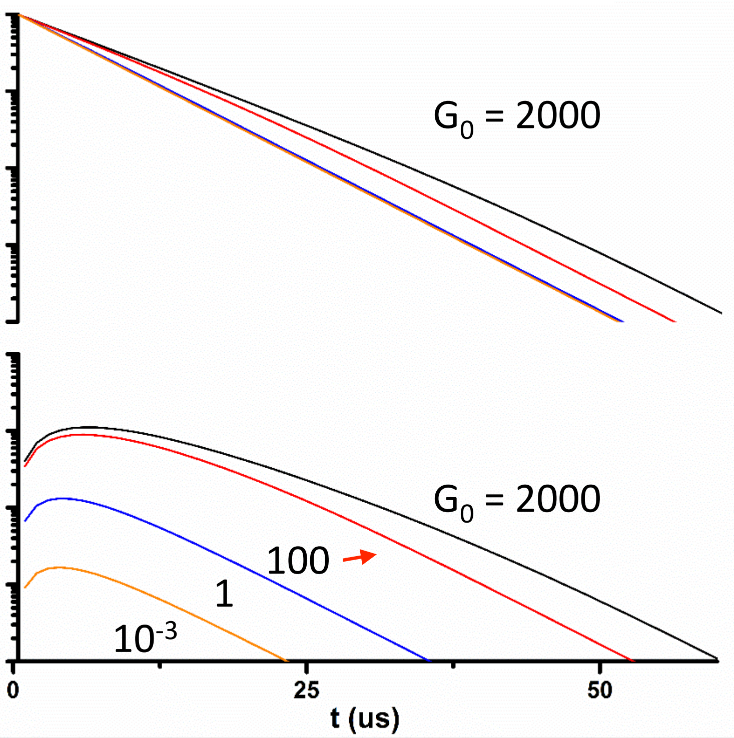

P_{sat}= Tw^2 hc$\Gamma_1\Gamma_2$k^3/(8πA$_{21}$) : saturation power
G_0 = P_{circ}/P_{sat} : saturation parameter

Γ_1: population relaxation rate
Γ_2: dephasing rate

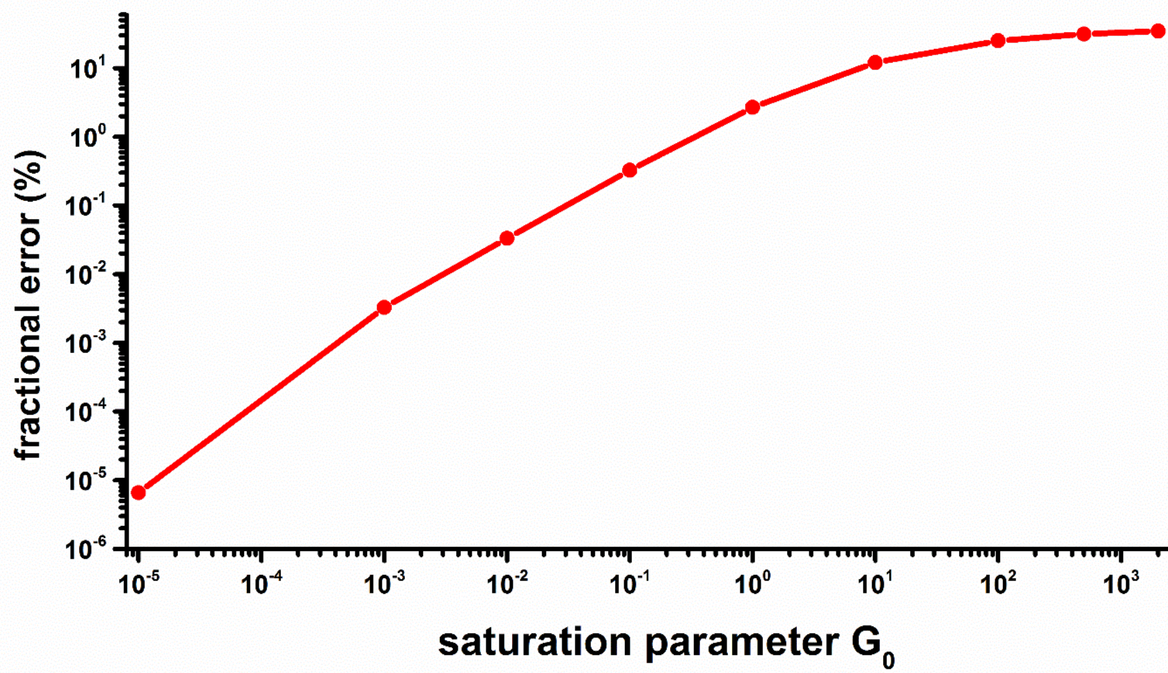

= 0.4
μs

Cancio et al, “Saturated-absorption cavity ring-down (SCAR) for high-sensitivity and high-resolution molecular spectroscopy in the mid-IR,,“ Chap. 4, Cavity-enhanced spectroscopy & sensing, eds. Gagliardi & Loock, p. 143 (2014).

Sensitivity of SCAR method

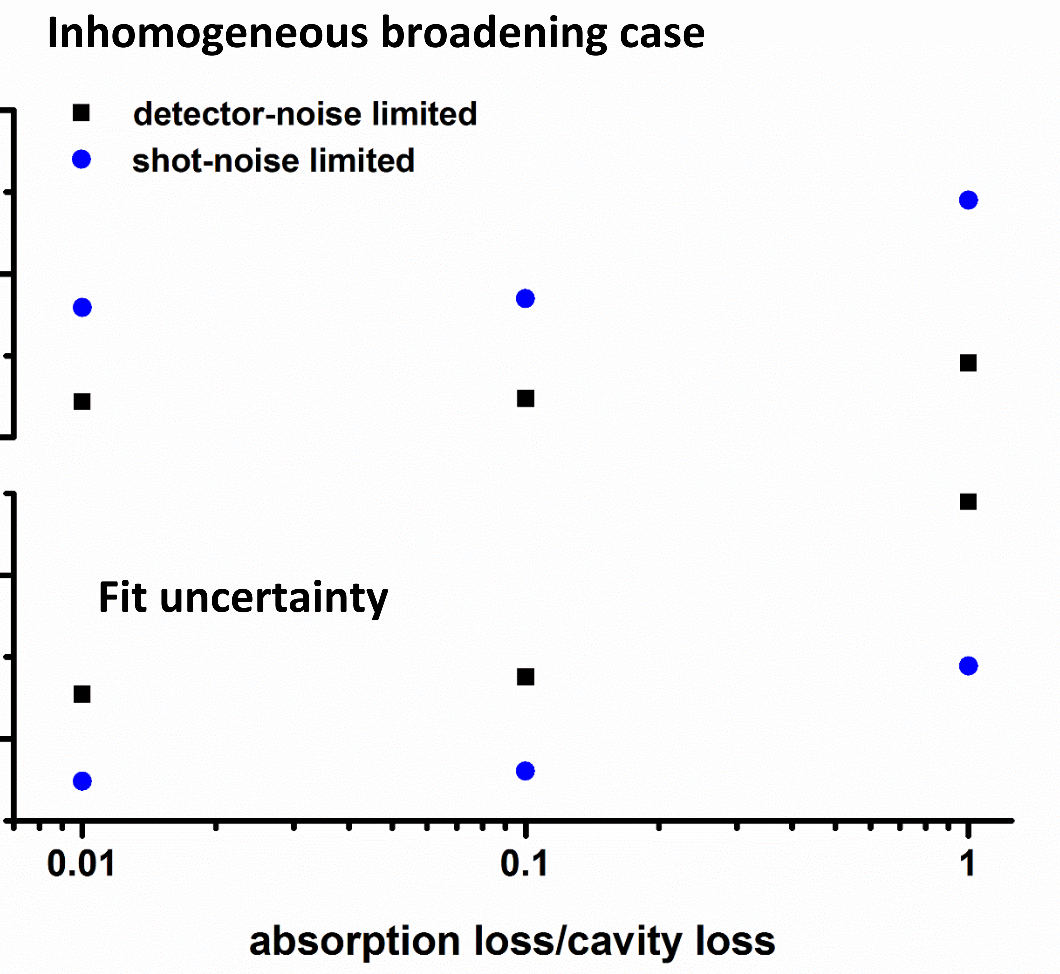

Theoretical advantage:
Can measure empty-cavity and absorption in a single decay

In practice:
Parameter correlations lead to relativel
uncertainties in fitted values

Must measure at optimal saturation parameter value, thus restricting useful range of the technique

Lehmann, Appl. Phys. B, "Theoretical detection limit SCAR & two-photon abs. CRDS, " **116**, 147-155 (2014)

Extinction ratio = 10 log(I_d/I_l)

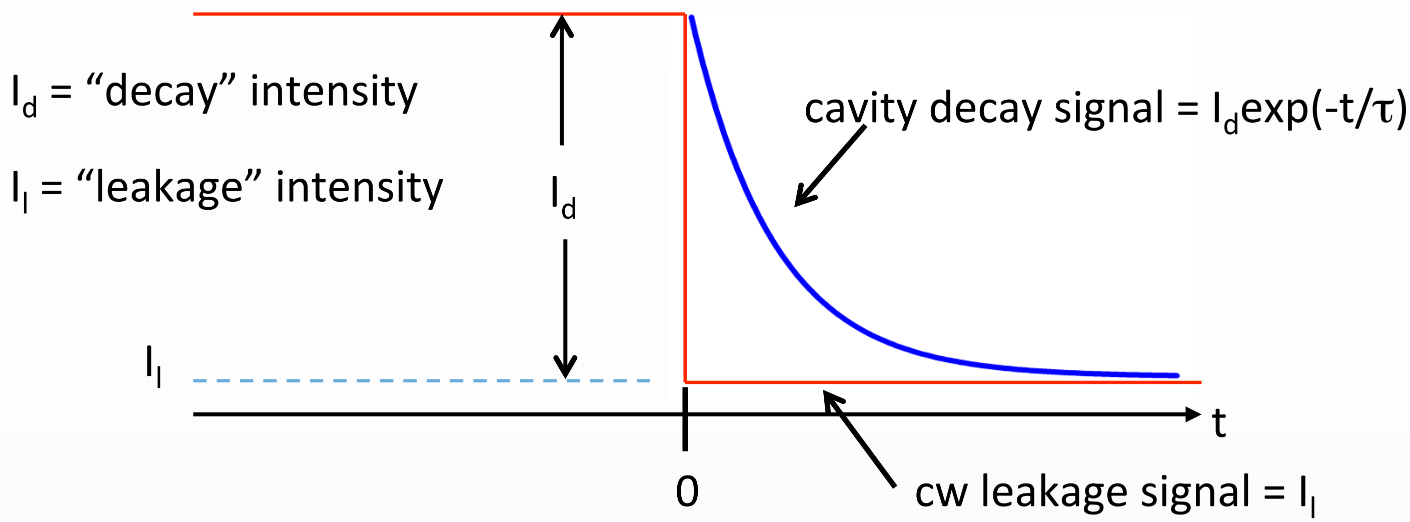

Ideal case (infinite extinction ratio): $I_l = 0$, ➔ exponential decay

Actual case:

leakage intensity interferes with decay signal to yield noisier and/or non-exponential decay

$$y(t) = y_0 + A[e^{-t/\tau} + 2\sqrt{I_l(t)/I_d}\, e^{-t/(2\tau)} + I_l(t)/I_d]$$

Effect of extinction ratio on the precision of measured τ

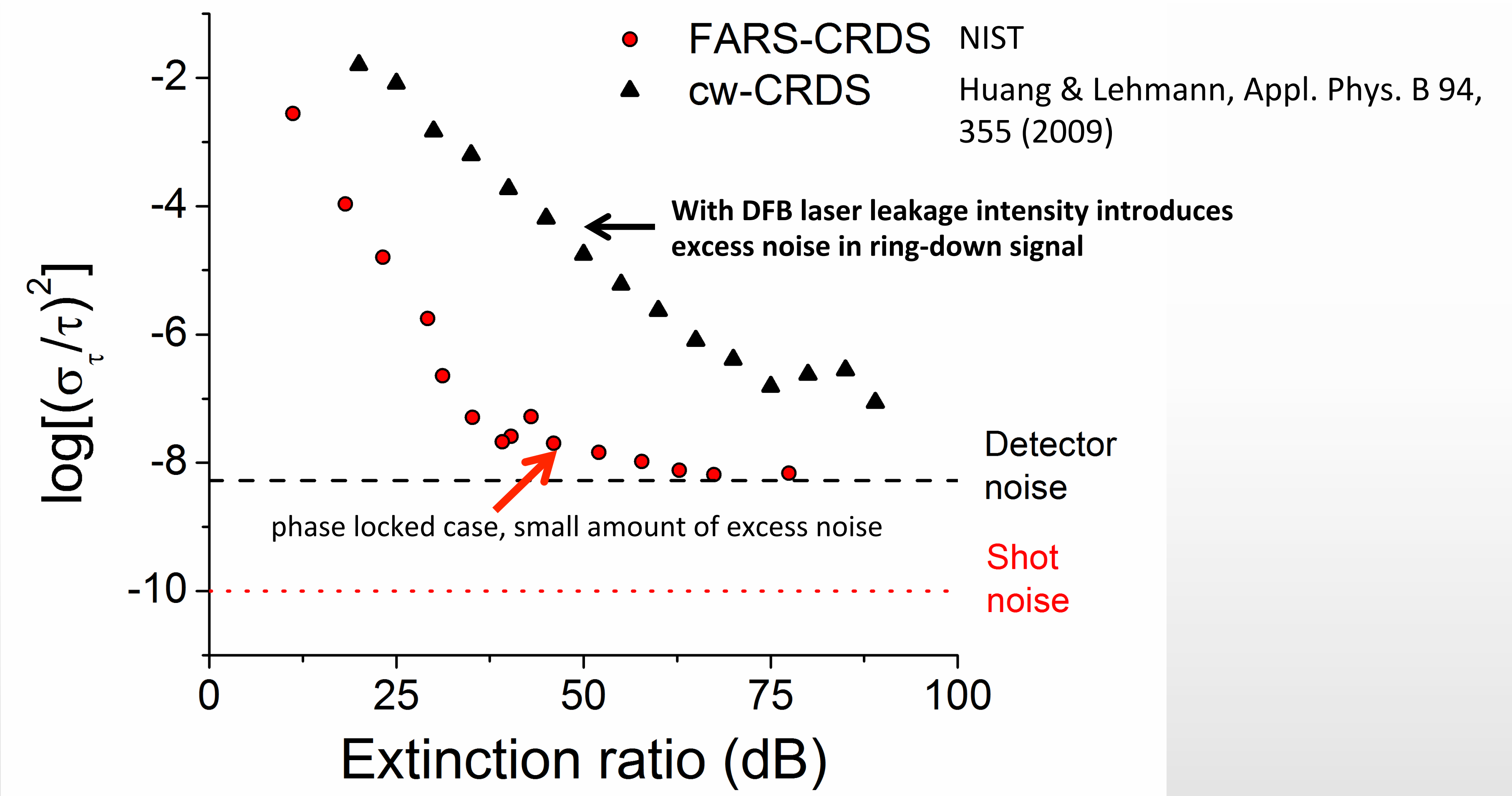

Coupled Cavities

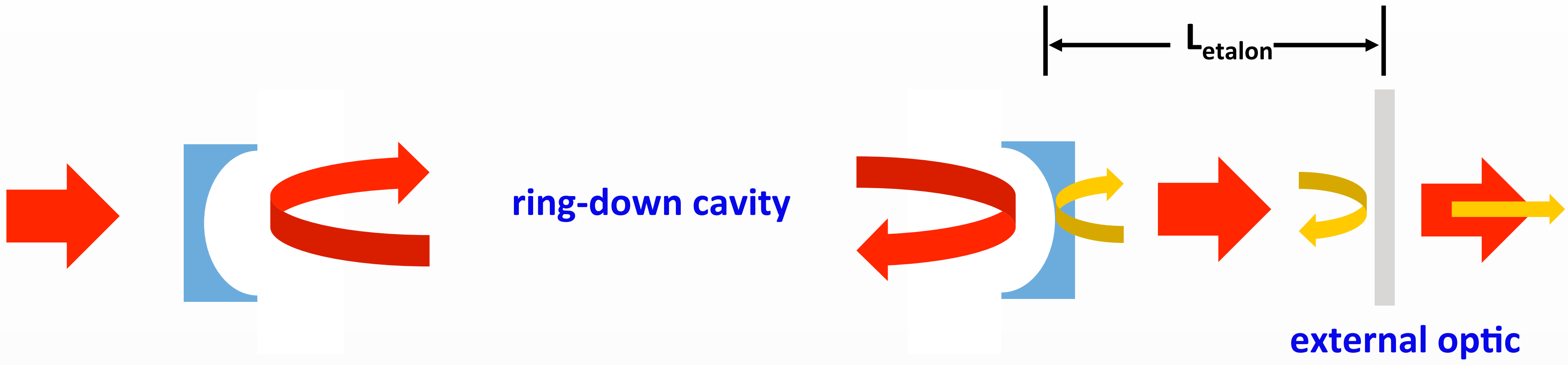

upled cavities ("etalons") are caused by reflections between normal incidence optics exterior to primary cavity and the nearest ring-down cavity mirror

ey lead to weak modulation of base losses with a spectrum period of $c/2L_{etalon}$

orly characterized, time-dependent etalons often limit the precision of CRDS spectral baselines

ey can be reduced using isolators, low-reflectivity optics and by tilting components

Assigning Etalons

Spectrum of empty-cavity losses

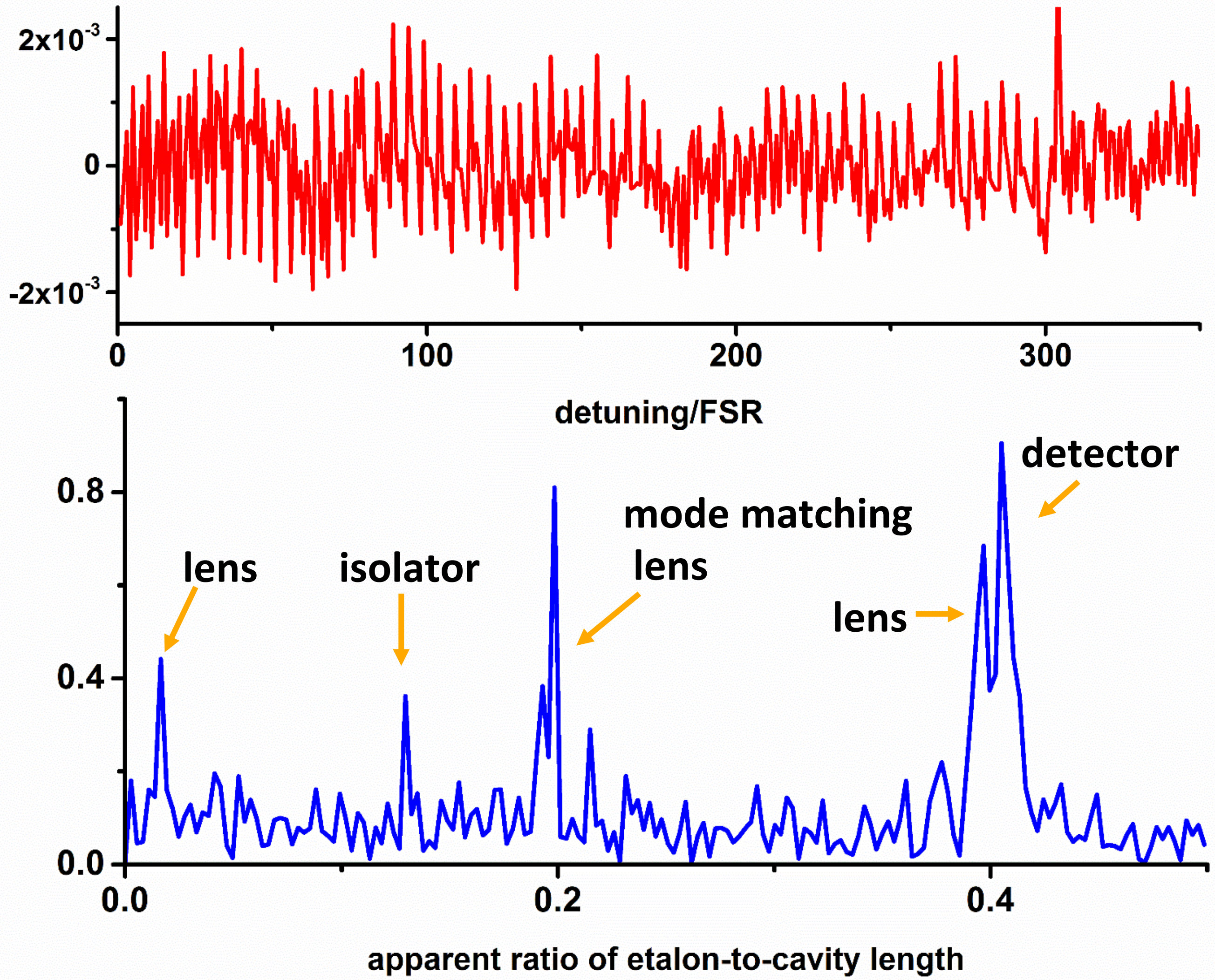

Aliasing Effect

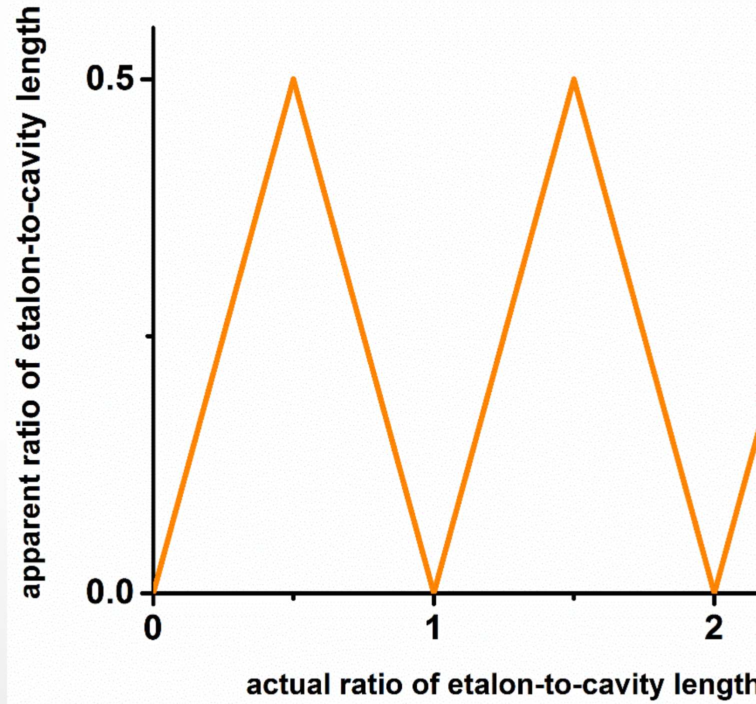

Drift in losses for a length-stabilized cavity

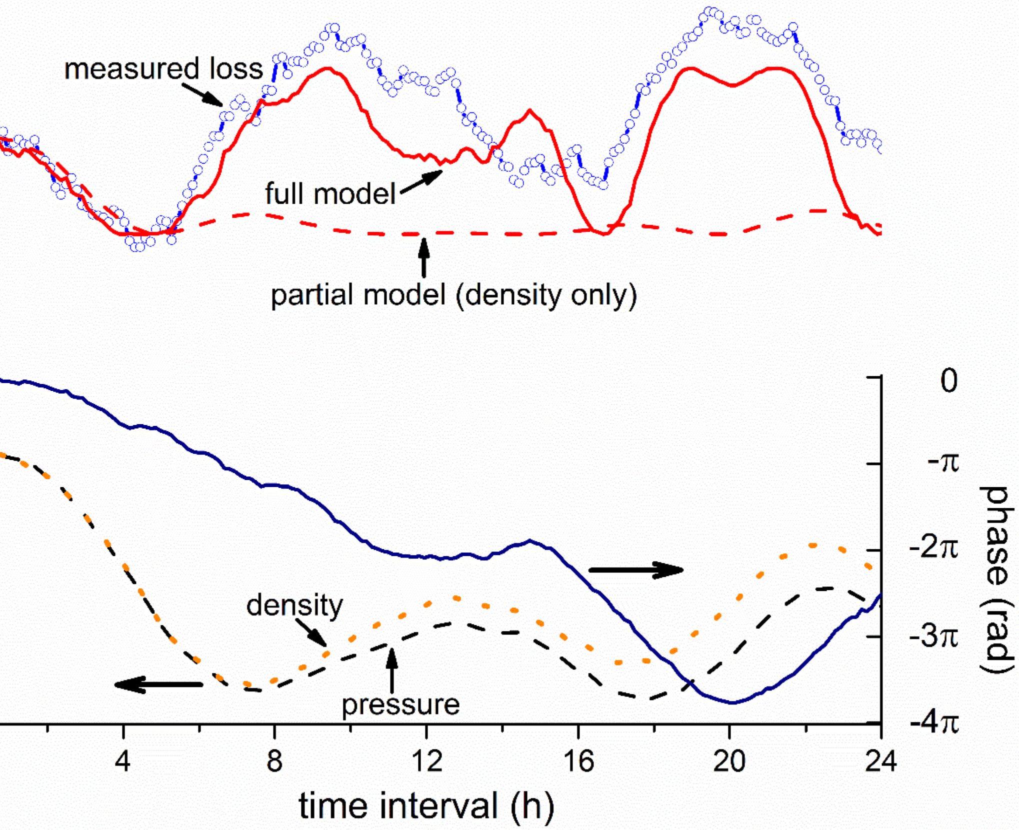

Modeled by <u>two</u> mechanisms:

Density dependent changes in refractive index of laboratory air

Thermal expansion of optical tabl

tois, Bielska and Hodges, “Differential CRDS,” JOSA B, **30**, 1486-1495 (2013).

Differential Cavity Ring-Down Spectroscopy

fixed reference mode[1]

$$\Delta L_q = L(\nu_q) - L(\nu_0)$$

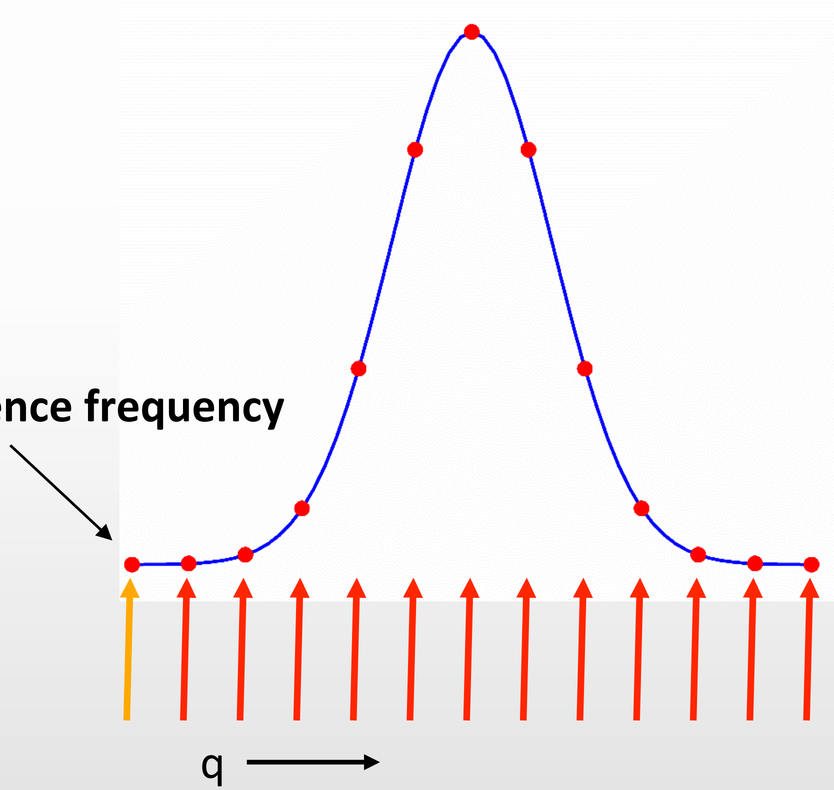

fixed frequency difference[2]

$$\Delta L_{q,q+\Delta q} = L(\nu_{q+\Delta q}) - L(\nu_q)$$

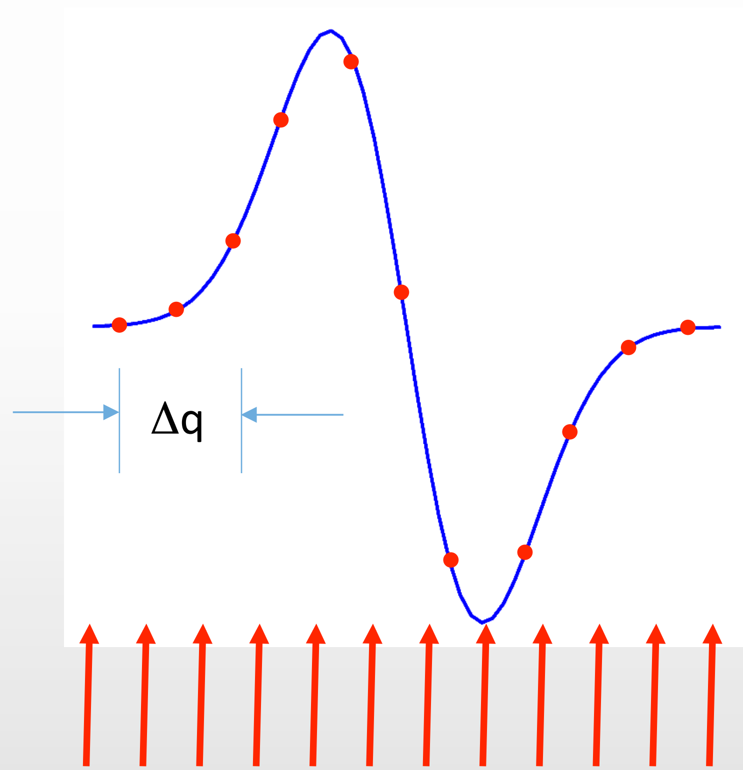

g & Lehmann, "Long-term stability in continuous wave cavity ringdown spectroscopy experiments", Appl. Opt. **49**, 1378-138

ois, Bielska and Hodges, "Differential cavity ring-down spectroscopy," JOSA B **30**, 1486-1495 (2013).

Improved signal-to-noise ratio (SNR) with differential-CRDS method

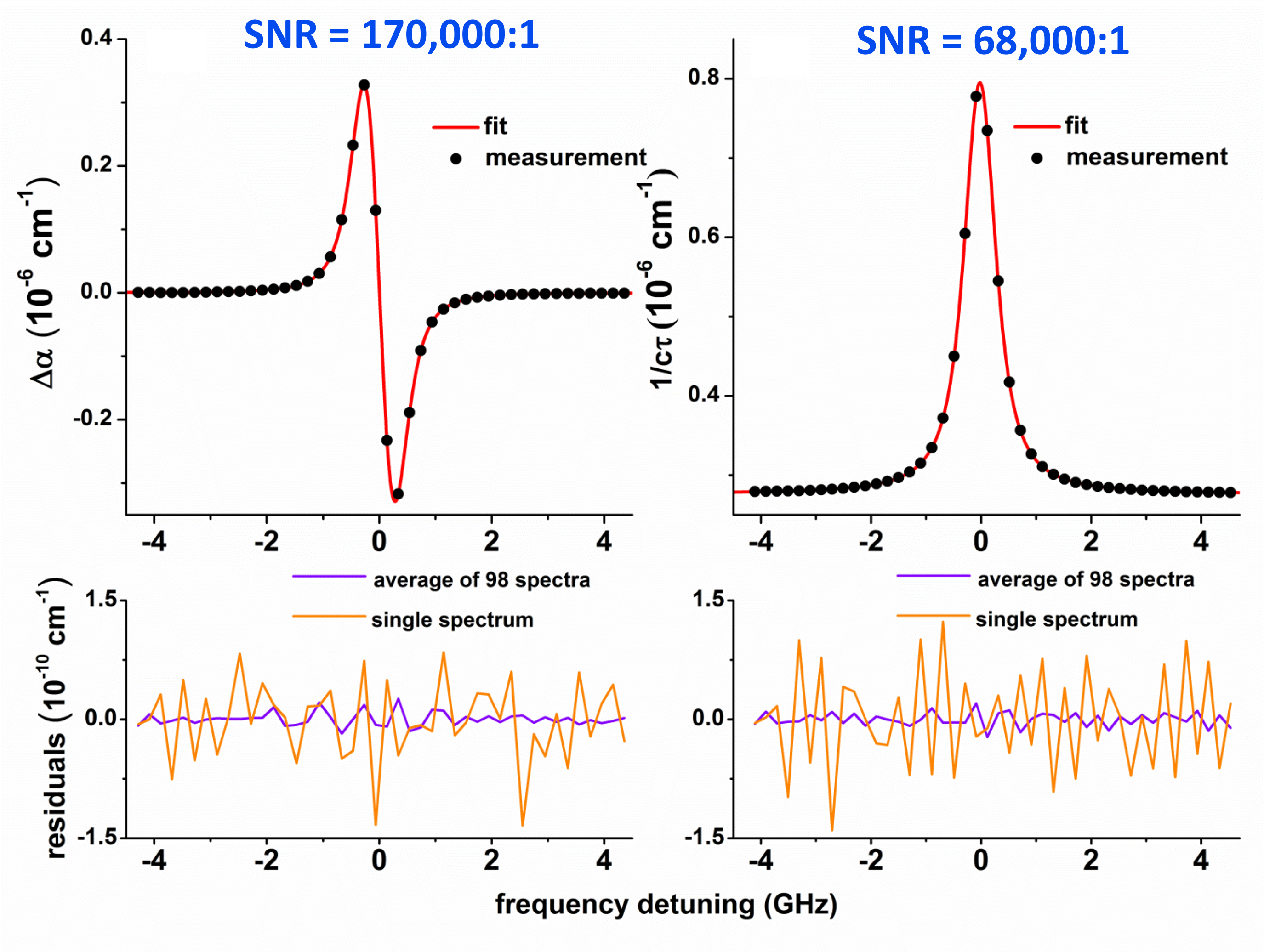

Etalon suppression with differential CRDS method

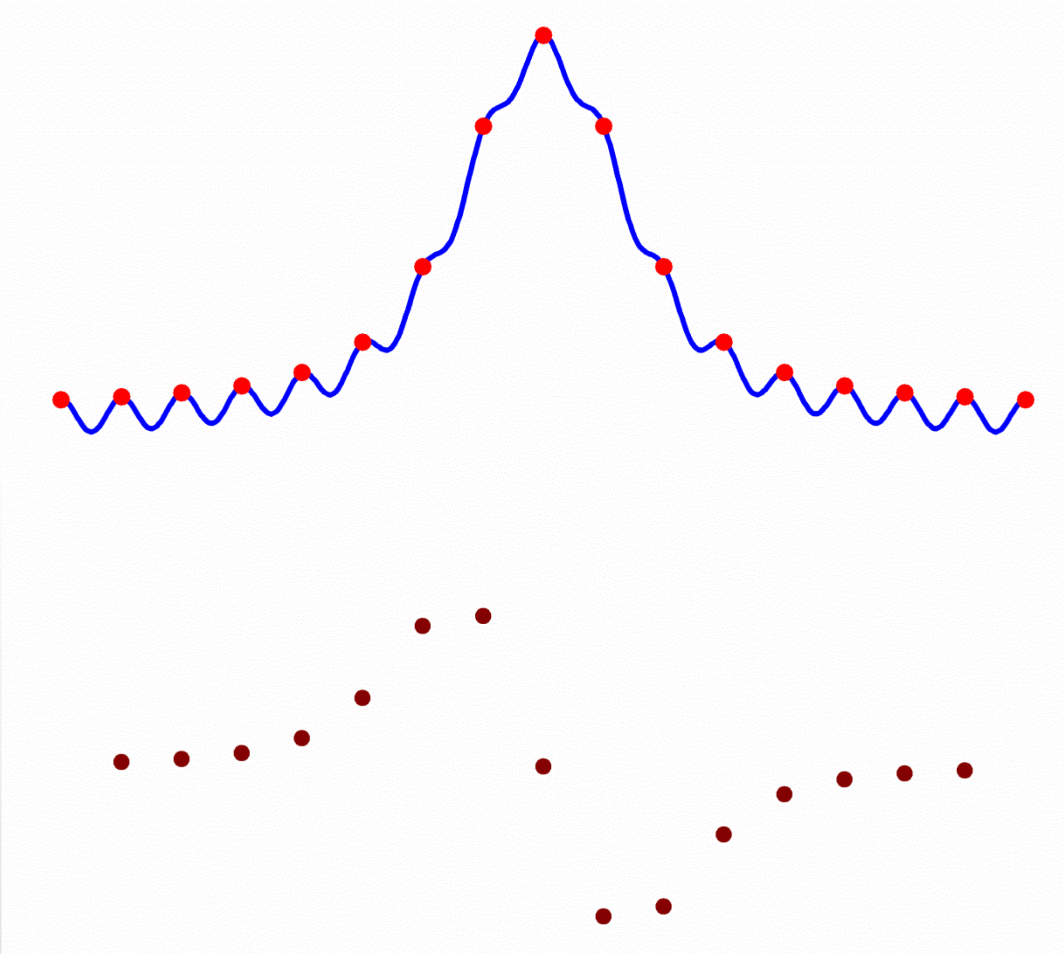

spectrum with baseline etalo

differential CRDS spectrum suppresses the etalon

Using Differential CRDS to compensate for changes in mirror losses: Scanned-cavity case

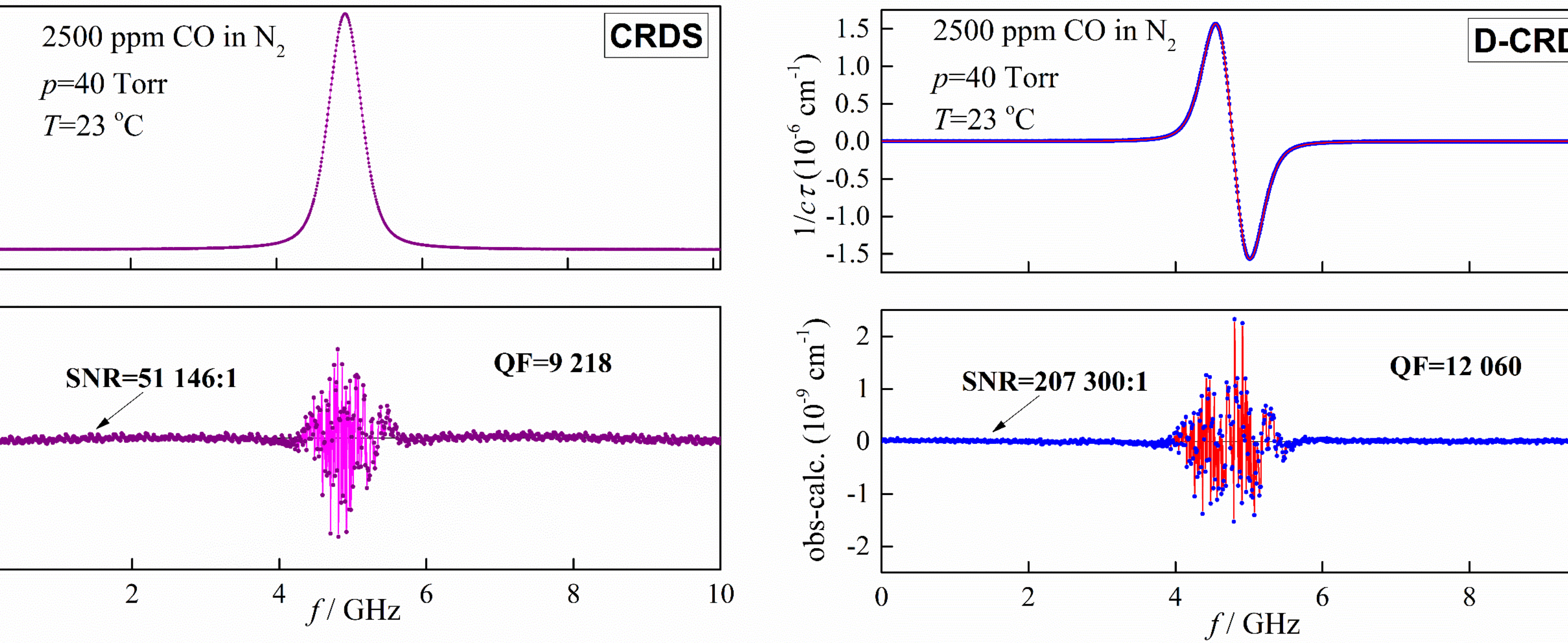

file: SDNGP

Measuring line shapes and intensities

Linking measured line parameters to the SI

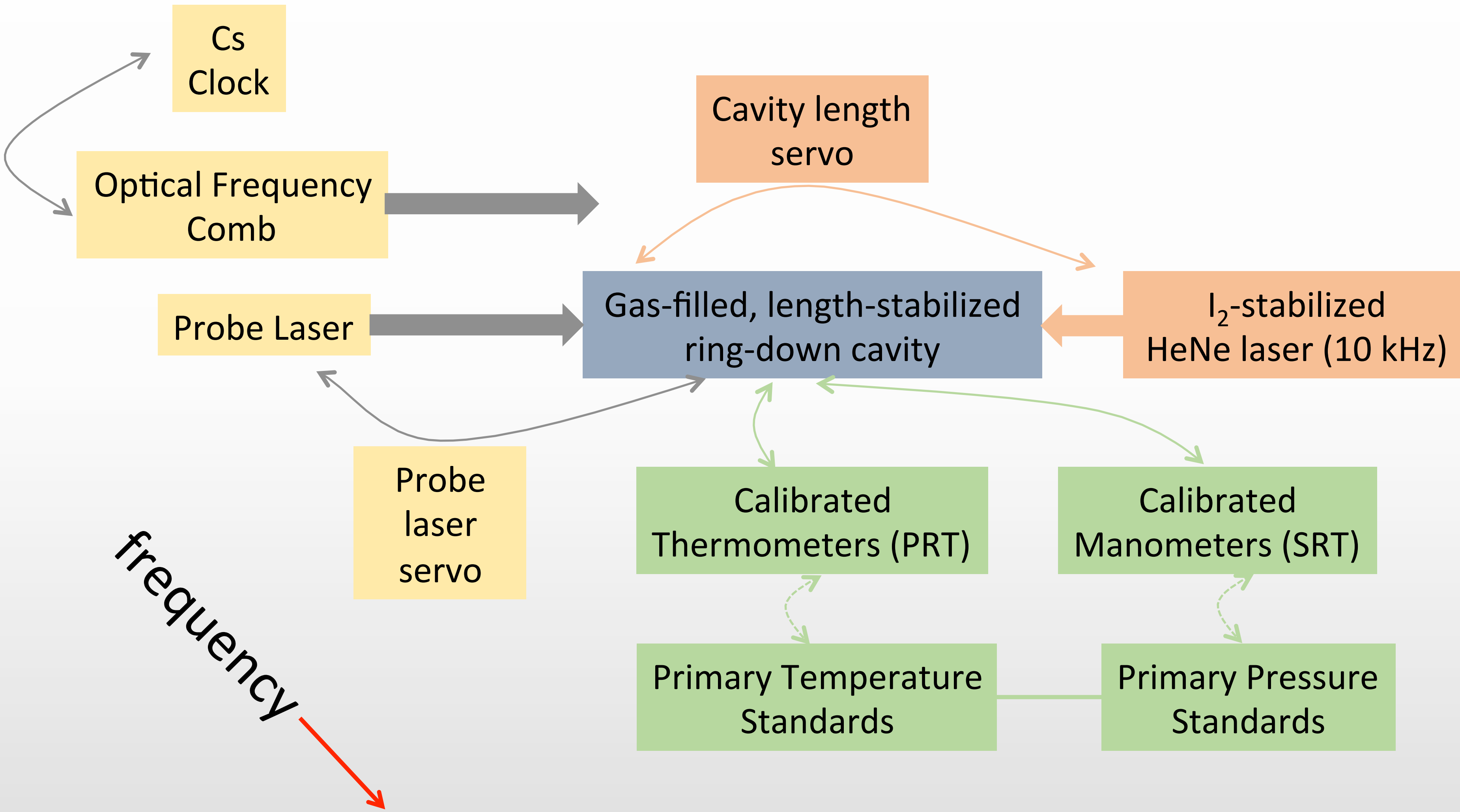

$$c\,\tau) = \alpha_0 + \alpha(\nu)$$

Measurement of Line Intensity (S) and Absorber Concentration (n)

$$S = \int \alpha(\nu)d\nu \,/\{\, n \int g(\nu)d\nu \} = A/n$$

measured absorption coefficient

line profile (unity area)

fitted spectrum area

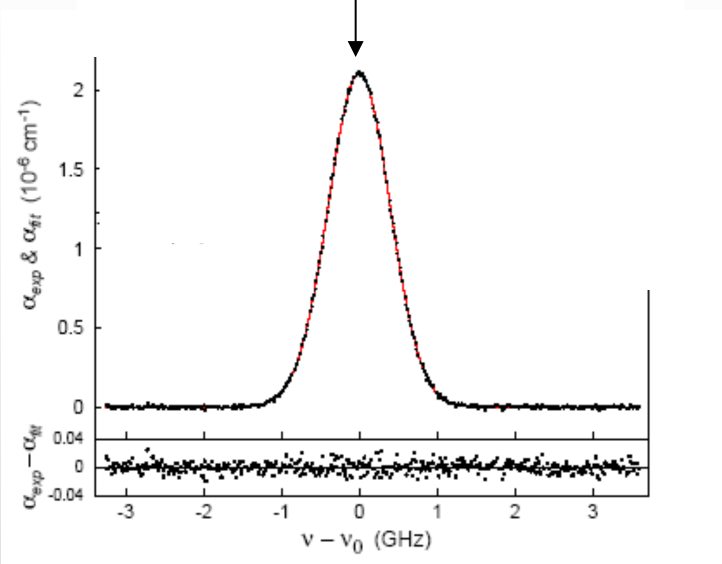

Once the intrinsic property ***S*** is known, then

$$n = A/S$$

Dependence of fitted line profile area: Voigt vs. Galatry (H_2O transitions, 1.28 um region)

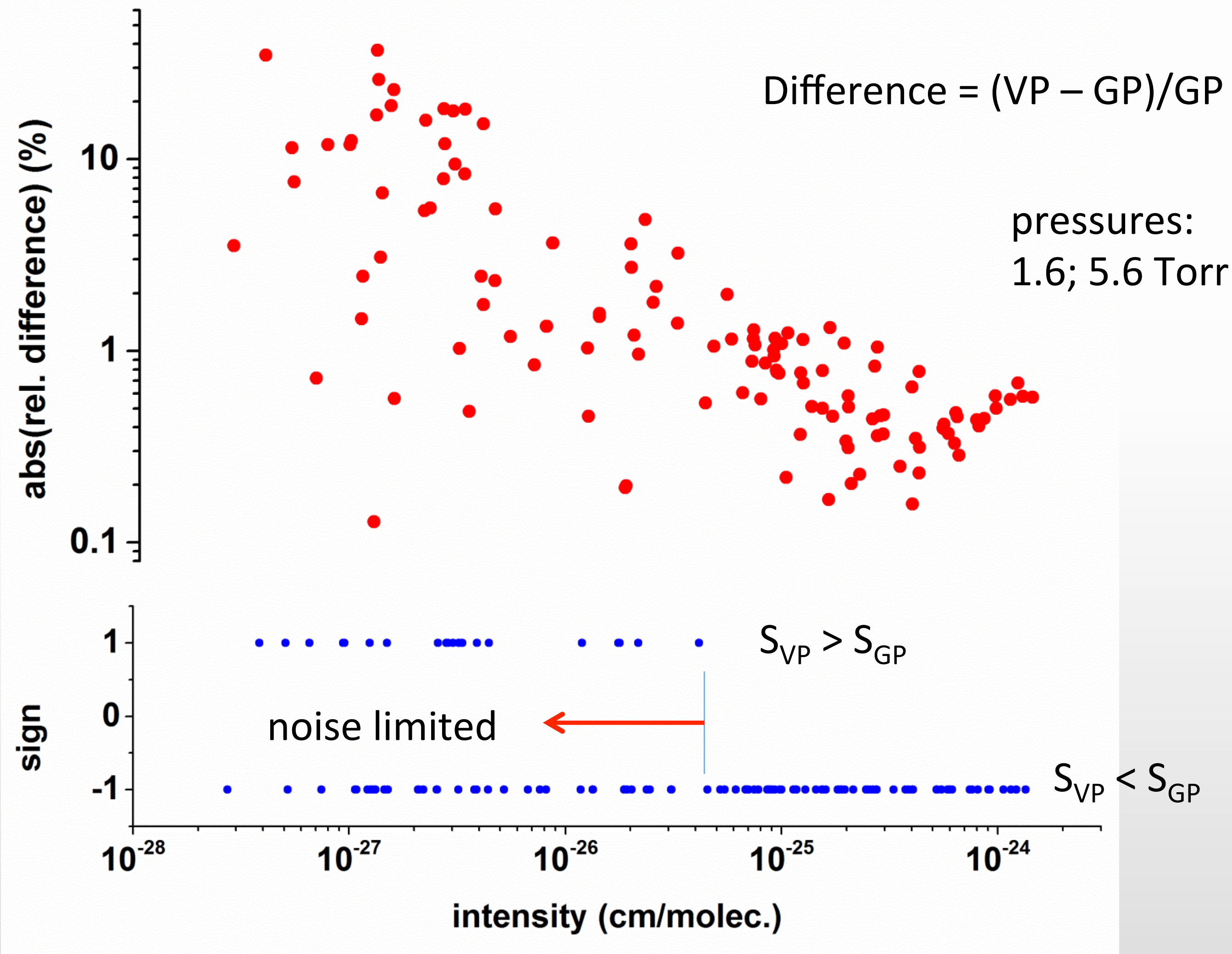

Voigt tends to underestimate line area

Partially correlated quadratic-speed-dependent Nelkin-Ghatak Profile
(Hartmann-Tran Profile)

$$\mathrm{DNG} = \frac{\tilde{I}_{\mathrm{qSDV}}(u; B_w\Gamma_0/\omega_D + \tilde{z})}{1 - \pi\tilde{z}\tilde{I}_{\mathrm{qSDV}}(u; B_w\Gamma_0/\omega_D + \tilde{z})}$$

Complex profile

$$\tilde{\nu}_{opt}/\omega_D = [\nu_{eff} - \eta(\Gamma_0 + i\Delta_0)]/\omega_D$$

Complex, normalized narrowing frequency

$$B_w(x) = 1 + a_w(x^2 - 3/2)$$

$$B_s(x) = 1 + a_s(x^2 - 3/2)$$

Quadratic approximation to speed dependence

Correspondence between pCqSDHC and pCqSDNGP parameters

$$a_w = \Gamma_2/\Gamma_0$$

$$a_s = \Delta_2/\Delta_0$$

$$Re[\tilde{\nu}_{opt}] = \nu_{vc} - \eta\Gamma_0$$

$$Im[\tilde{\nu}_{opt}] = -\eta\Delta_0$$

hanisms: 1) collisional narrowing (hard-collision model), 2) speed-dependent broadening and shifting,
artial correlations between velocity-changing and dephasing collisions

H_2O line shape study

single-spectrum fit

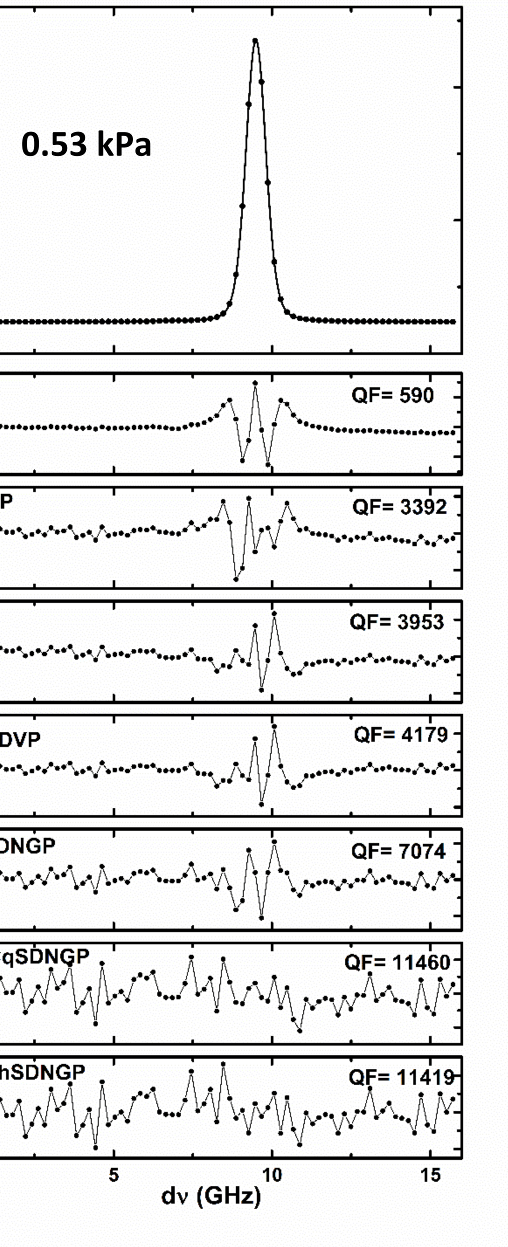

Need to include:

1. collisional narrowing
2. speed dependent effects
3. partial correlation between velocity-changing and dephasing collisions

7892.3021 cm $^{-1}$
S = 1.89x10^{-25} cm molec.$^{-1}$
(002)- (000)
(15 5 6) – (9 2 7): Q' – Q''

7799.9970 cm $^{-1}$
S = 2.58x10^{-25} cm molec.$^{-1}$
(002) - (000)
(10 4 6) – (9 3 7): Q' – Q''

multi-spectrum fit

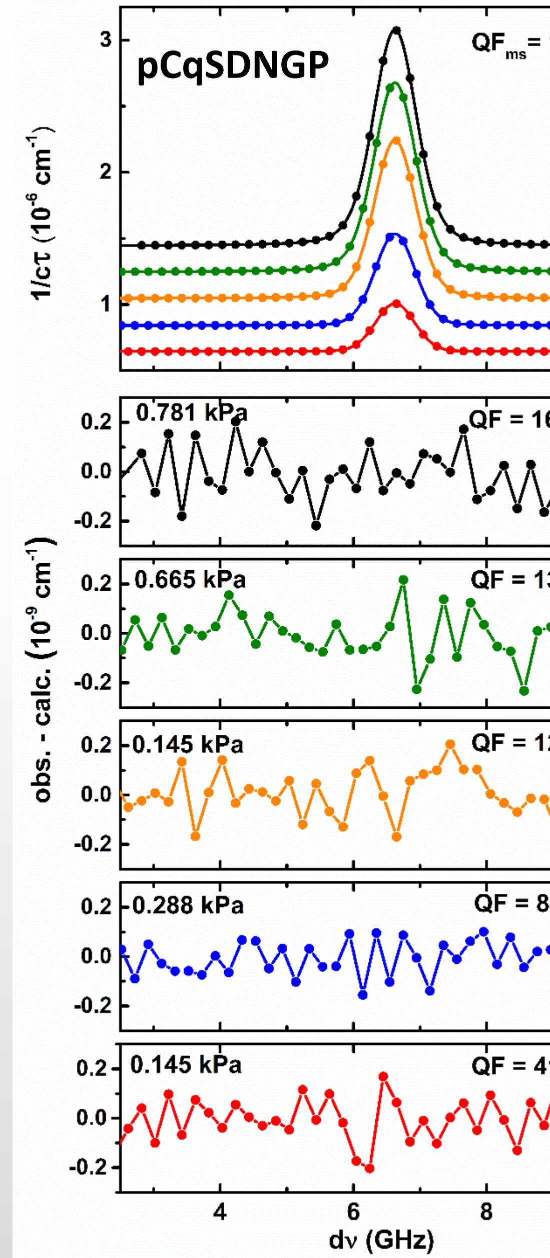

High precision line shape measurements

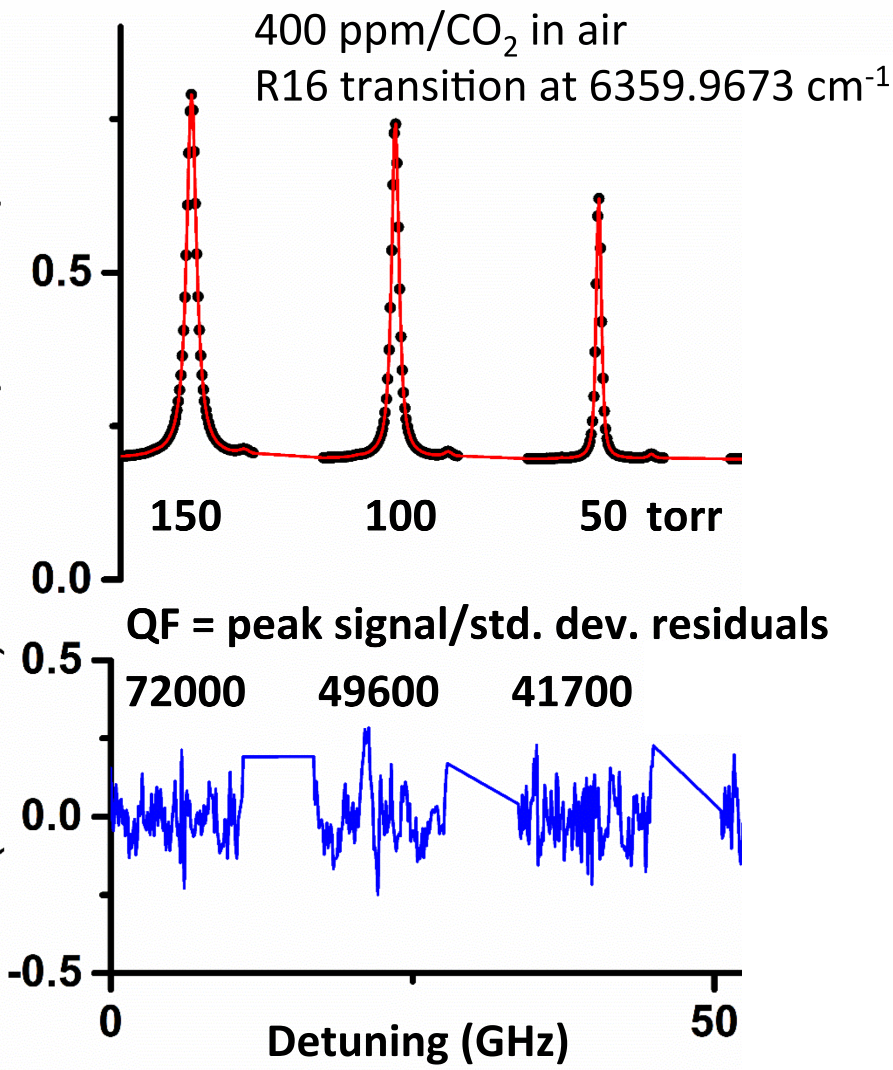

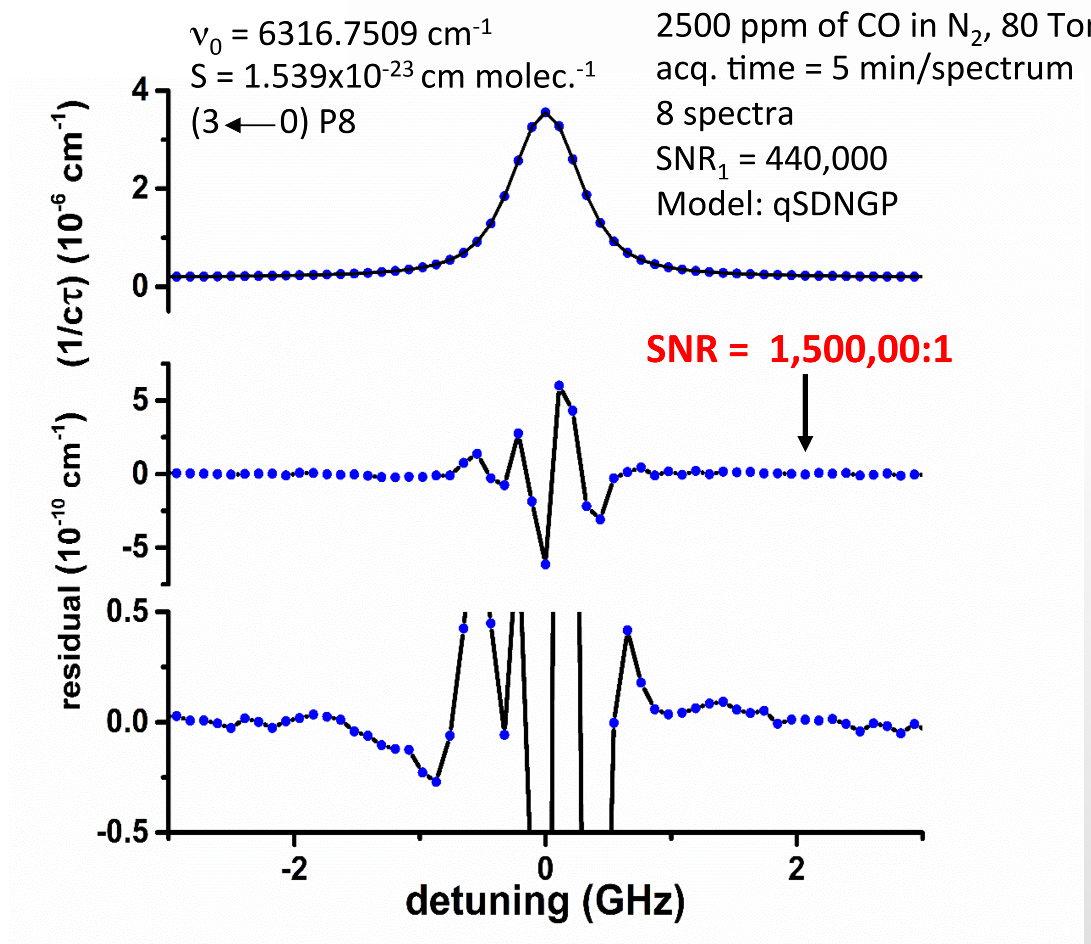

ensitivity of multispectrum fits to error in pressure measurement

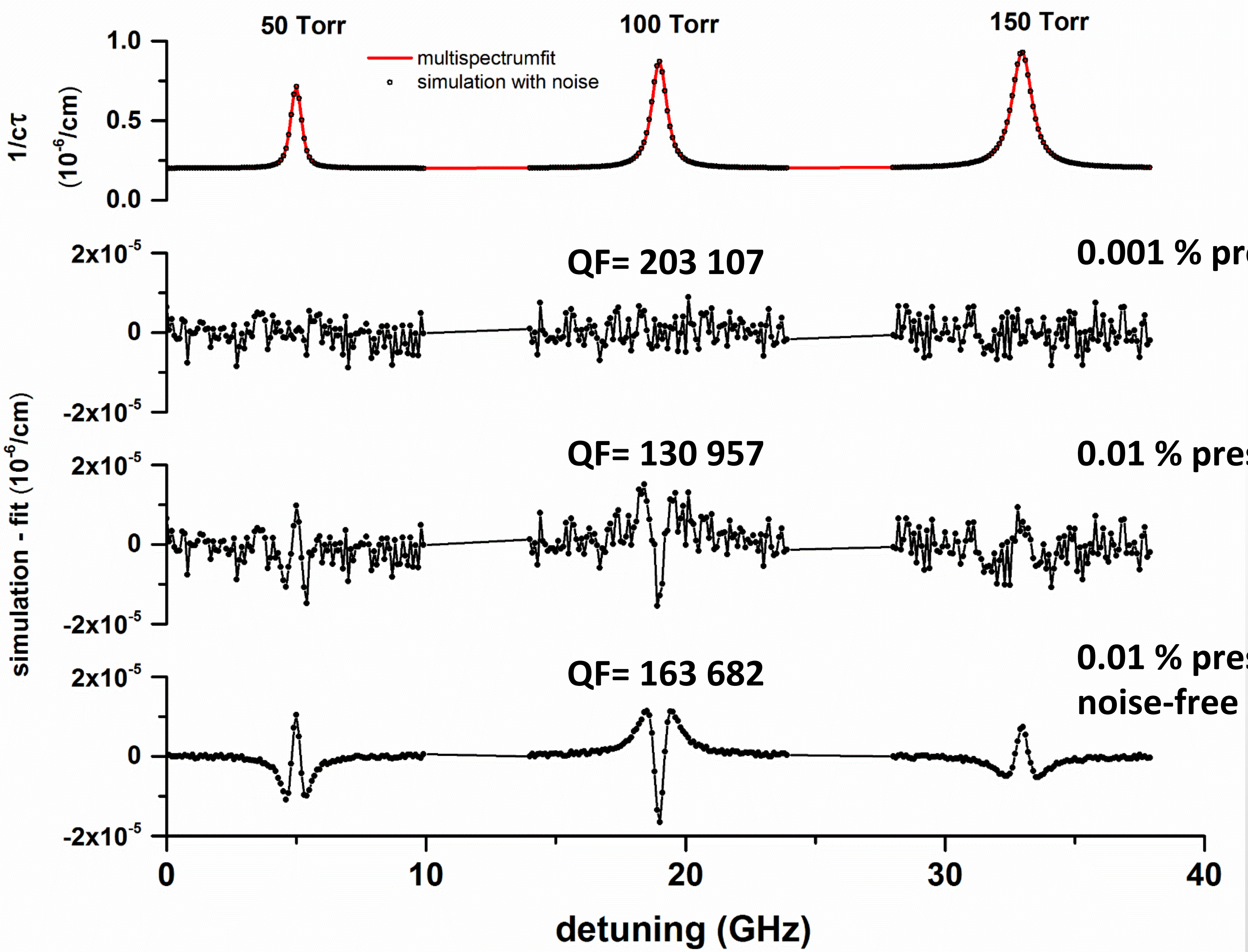

Simulatio

0.001 % pressure error

0.01 % pressure error

0.01 % pressure error
noise-free absorption

CO_2-in-air sample preparation

Need steady flow of sample ga[s to]
mitigate wall effects

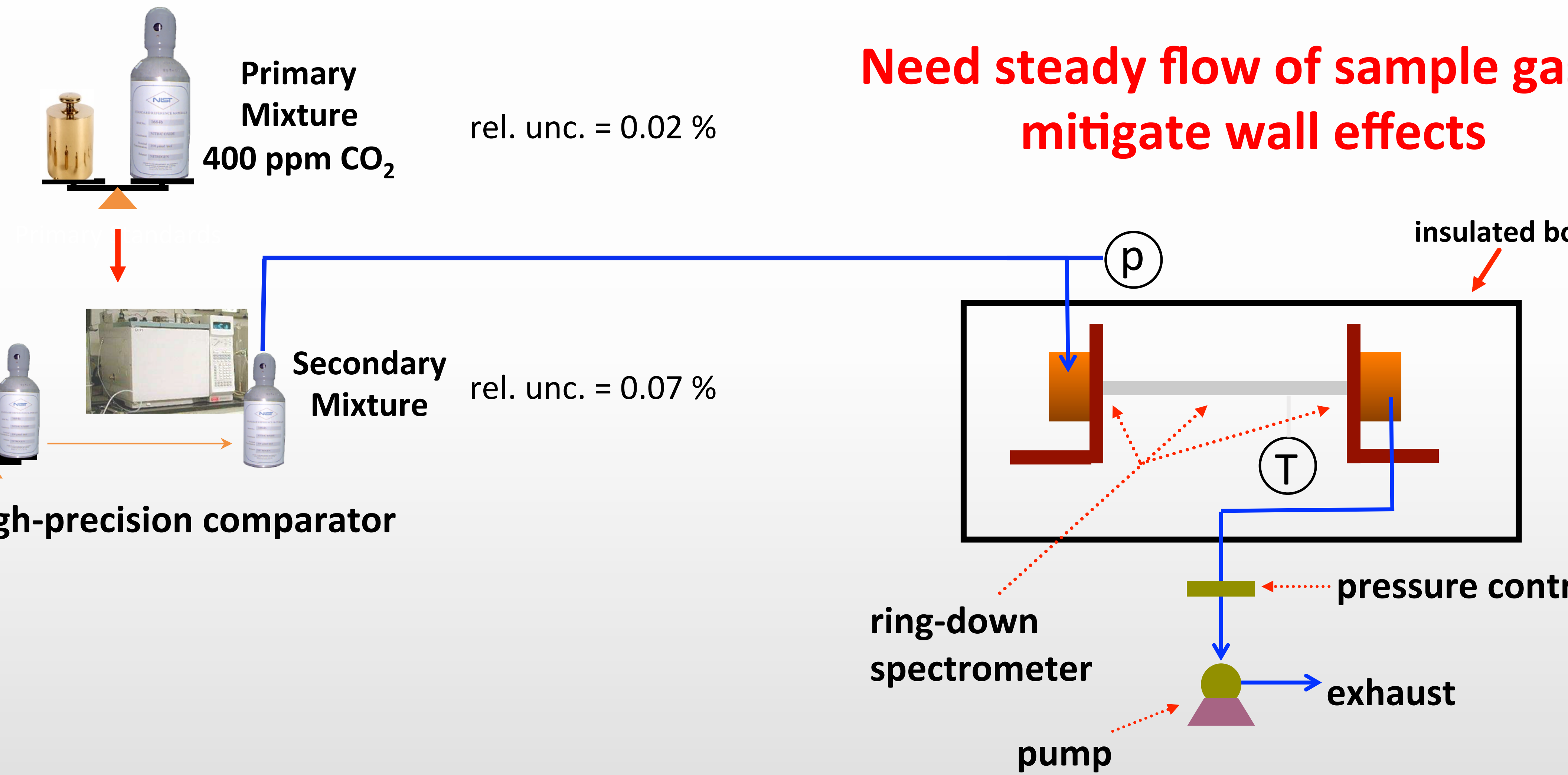

CO_2 outgassing effects

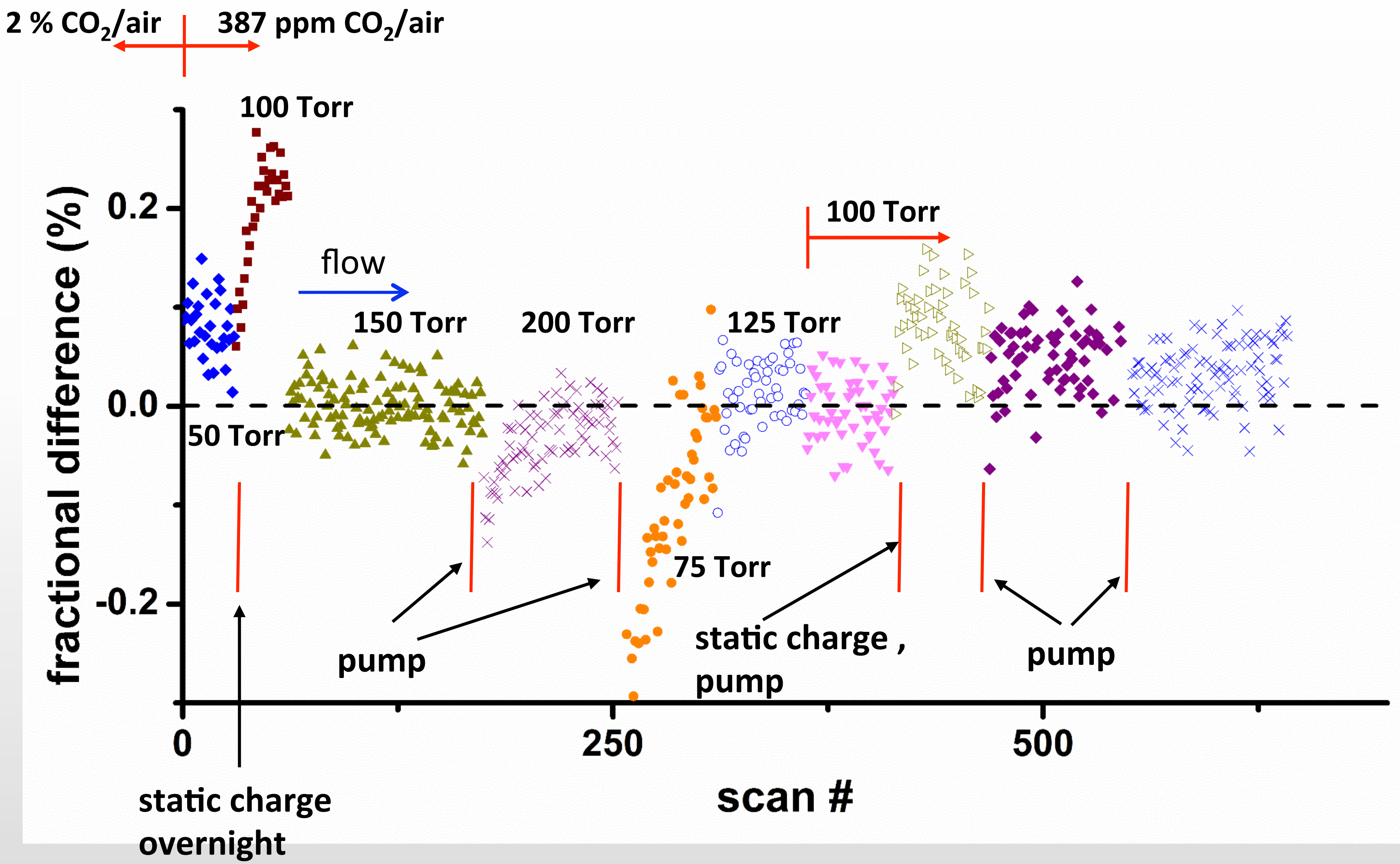

Accuracy of CO_2 intensity measurements: 1.6 um region

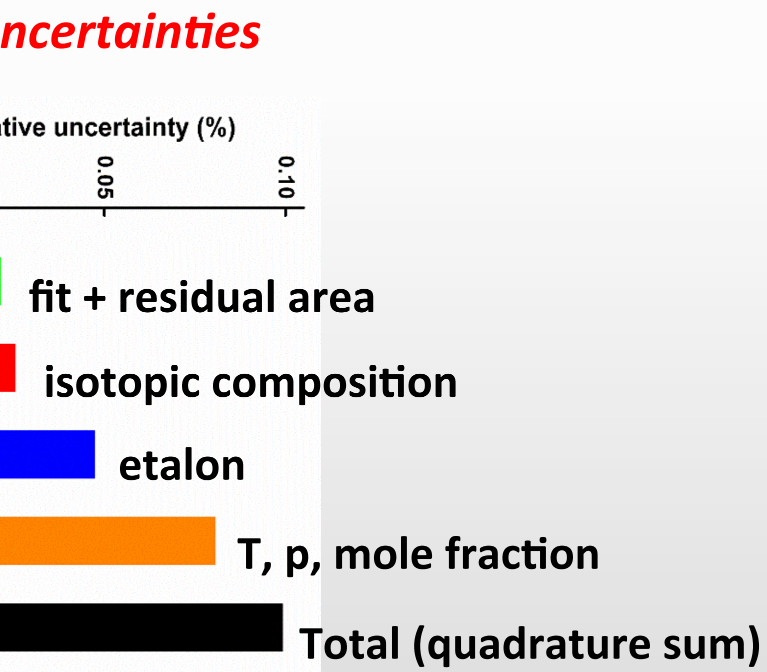

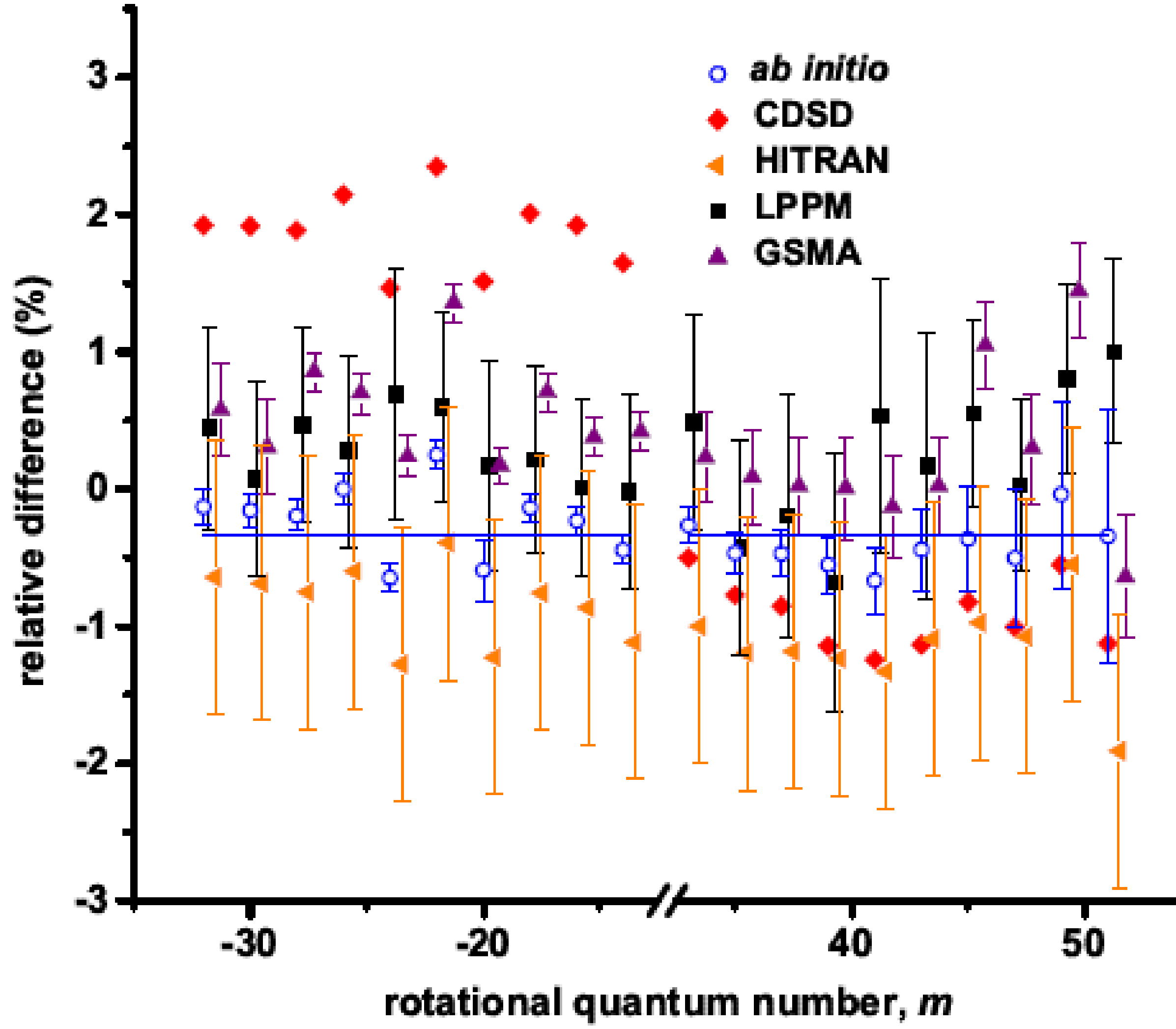

Polyansky et al., "High-accuracy CO_2 line intensities determined from theory and experiment," Phys. Rev. Lett. (2015)

New measurement strategies

Frequency-agile, rapid scanning (FARS) spectroscopy

Method:

- Use waveguide electro-optic phase-modulator (PM) to generate tunable sidebands
- Drive PM with a rapidly-switchable microwave (MW) source
- Fix carrier and use ring-down cavity to filter out all but one selected side band

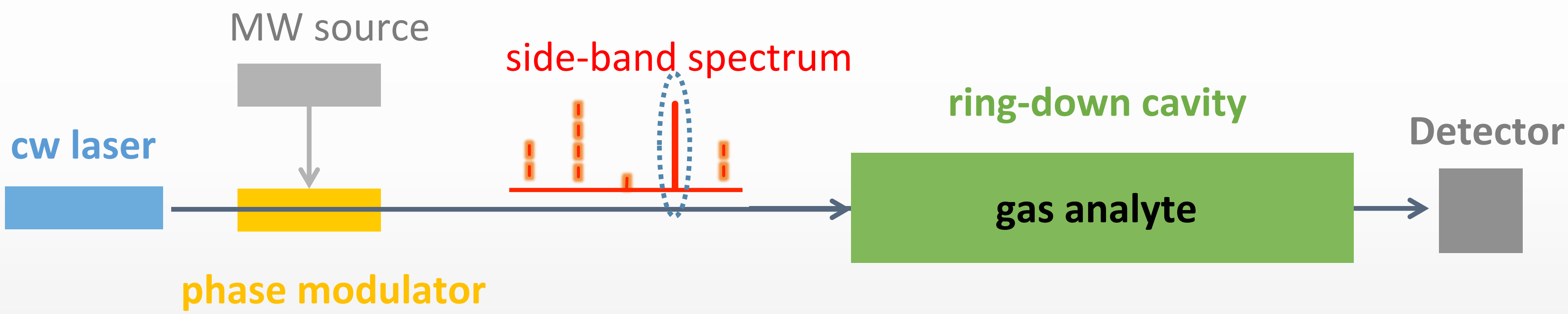

Advantages:

- Overcomes slow mechanical and thermal scanning
- Links optical detuning axis link to RF and microwave standards
- Wide frequency tuning range (> 90 GHz = 3 cm^{-1})

nature photonics LETTERS
PUBLISHED ONLINE: 28 APRIL 2013 | DOI: 10.1038/NPHOTON.2013.98

Frequency-agile, rapid scanning spectroscopy

G.-W. Truong[1,2], K. O. Douglass[1], S. E. Maxwell[1], R. D. van Zee[1], D. F. Plusquellic[1]*, J. T. Hodges[1] and D. A. Long[1]*

FARS measurement principle

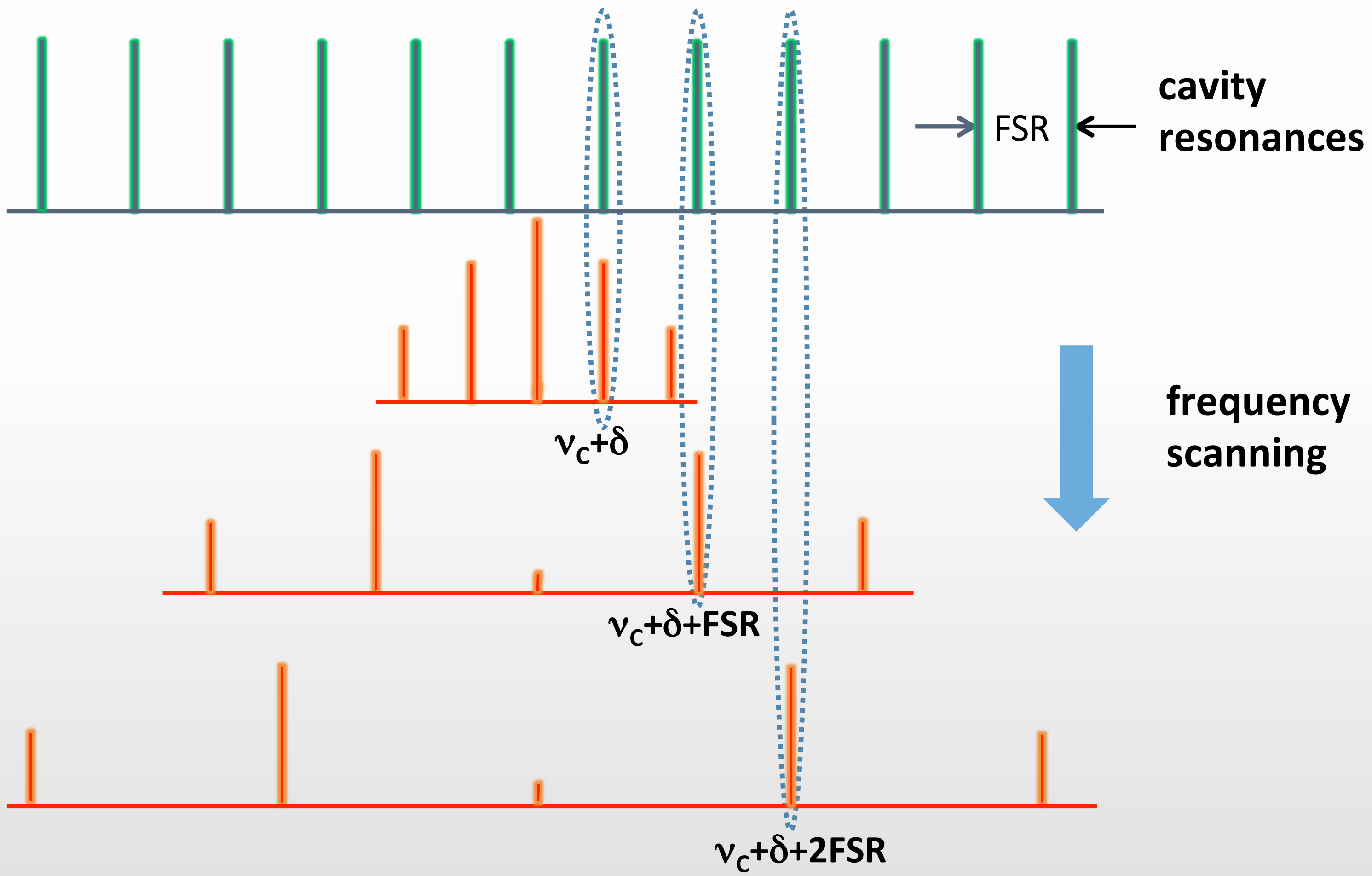

Averaging Statistics: Standard FARS-CRDS vs. Differential FARS-CRDS

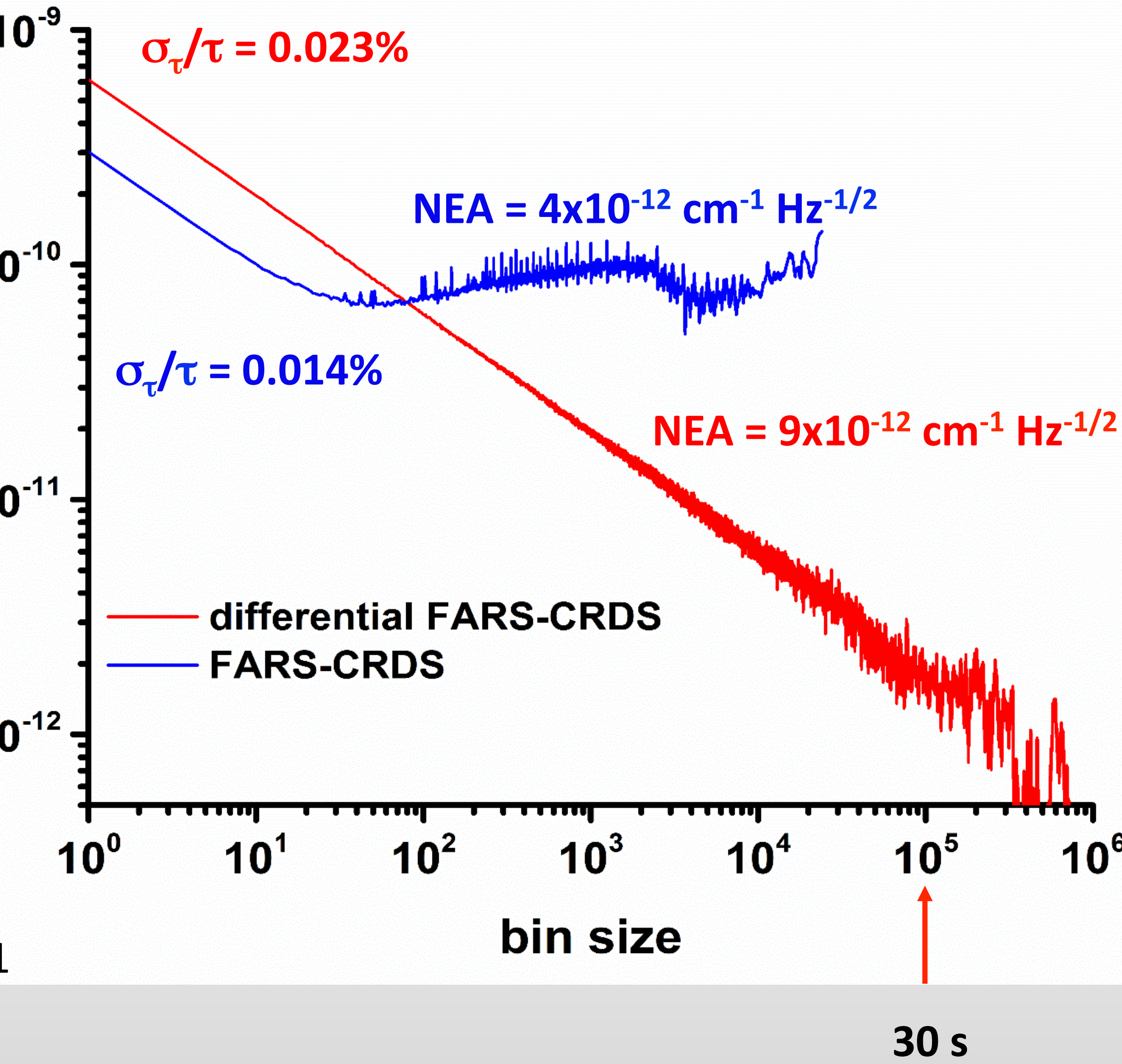

Differential approach increases opti
averaging time by more than three c
of magnitude

FARS-CRDS with OFC-referenced frequency axis

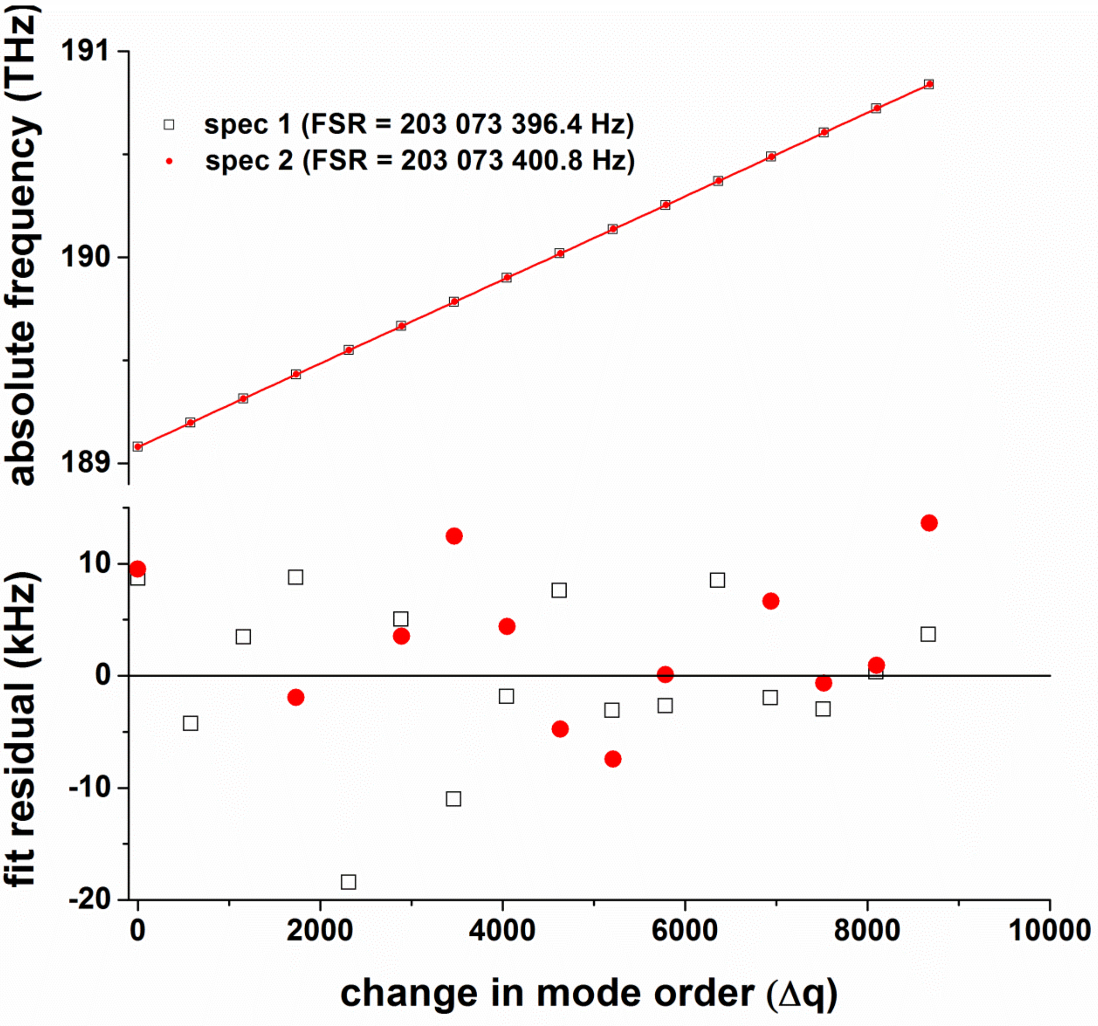

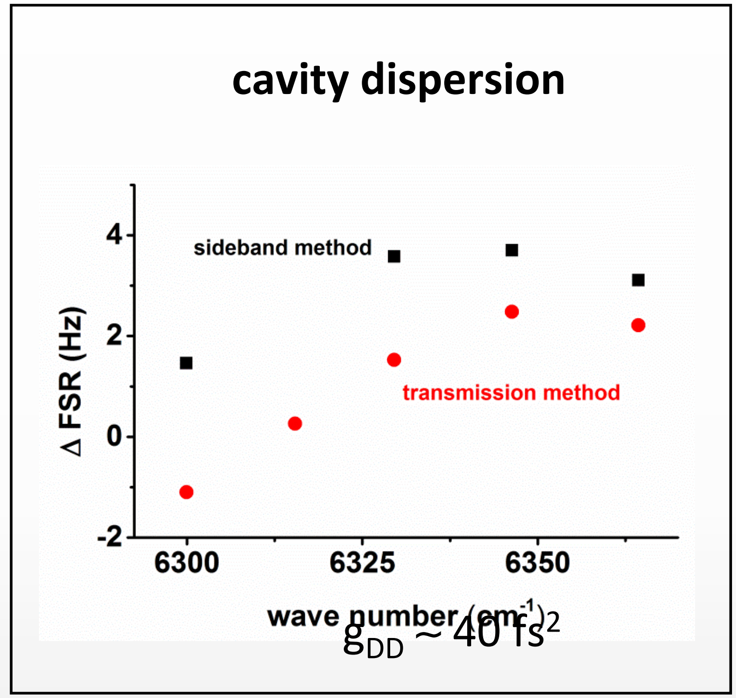

$g_{DD} \sim 40\ fs^2$

System includes:

Ring-down cavity locked to I_2-stabilized HeNe

Probe laser PDH-locked to cavity

Optical frequency comb (OFC) for absolute ref

FARS eliminates "dead-time" in CRDS scans

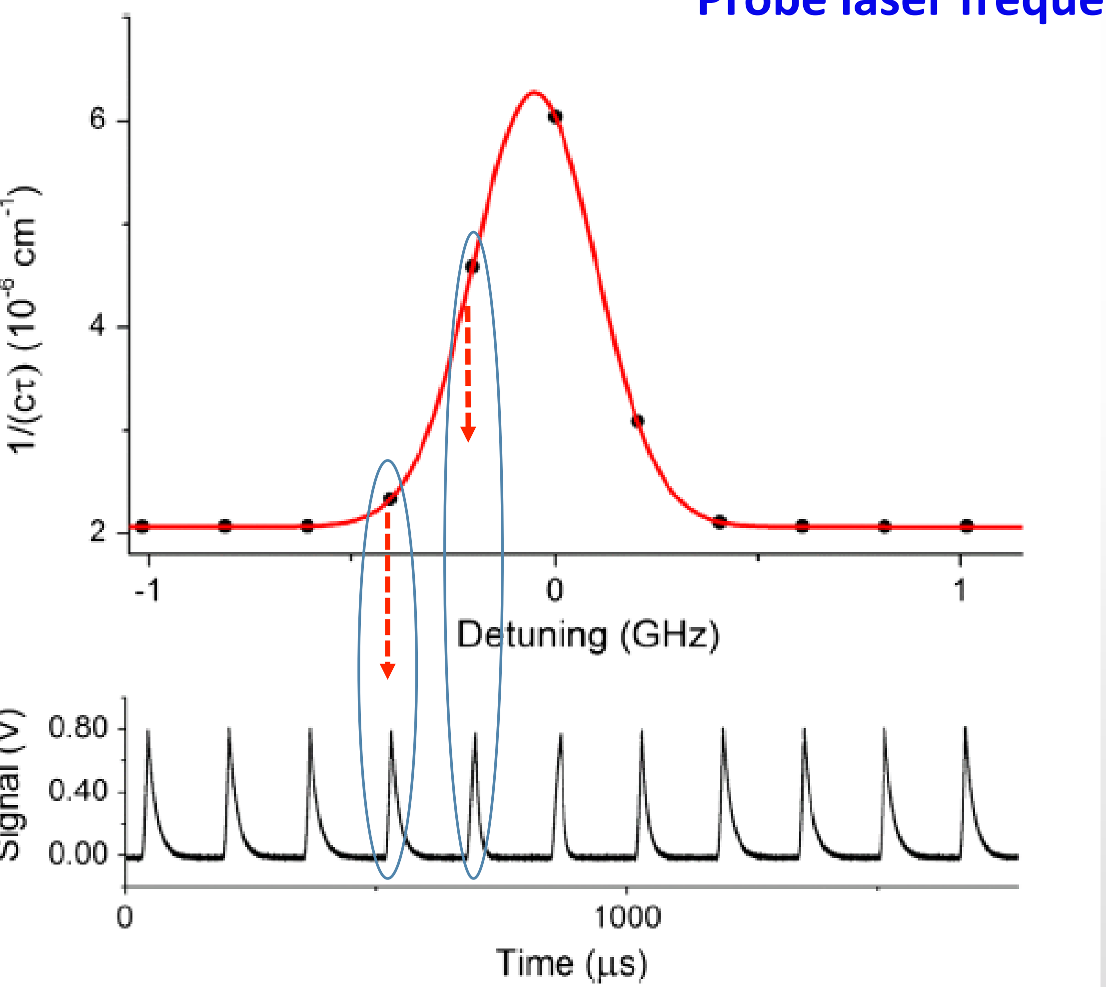

Probe laser frequency can be tuned and relocked to next cavity r during the previous decay event

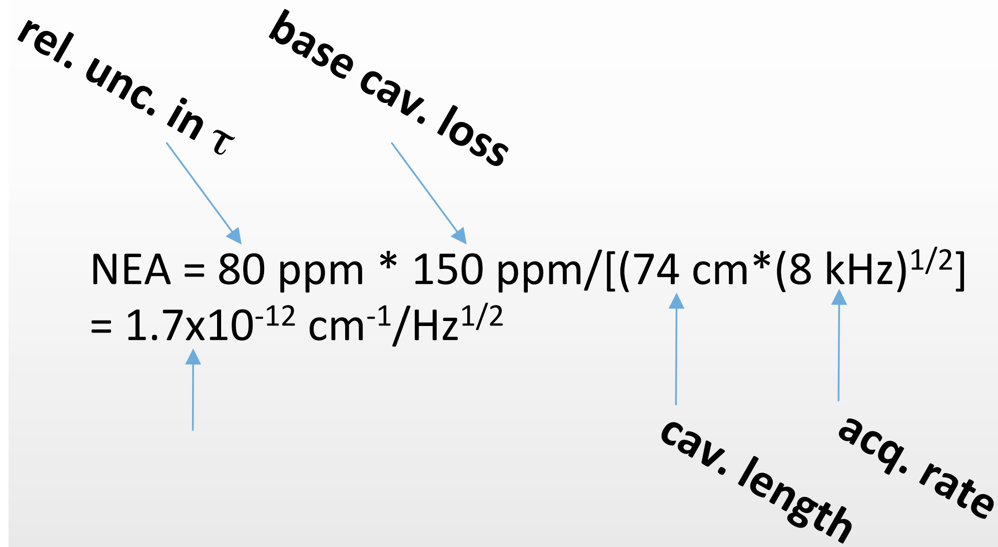

NEA = 80 ppm * 150 ppm/[(74 cm*(8 kHz)$^{1/2}$]
= 1.7x10^{-12} cm^{-1}/Hz$^{1/2}$

Long et al., *Frequency-agile, rapid scanning spectroscopy: absorption sensitivity of 2x10^{-12} cm^{-1} Hz$^{-1/2}$ with a tunable diode*
Appl. Phys. B **114**, 489-495 (2014)

Measuring losses in terms of cavity line width

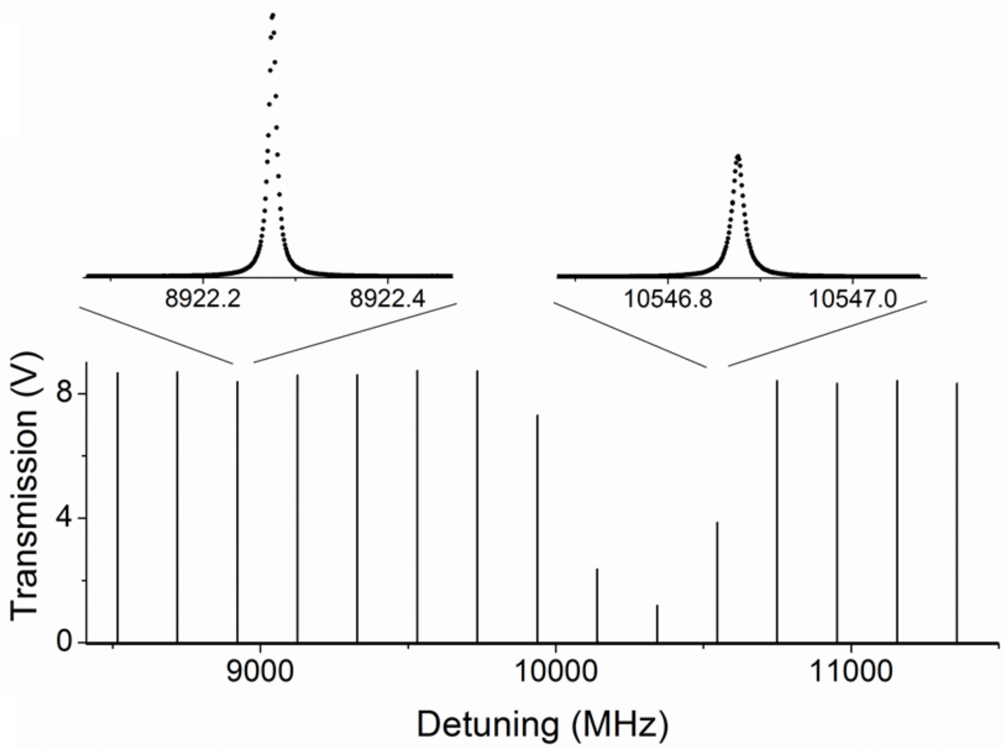

With PDH-locked FARS-CRDS can measure the shape and width of individual cavity resonances

The width of the resonances provides an equivalent measure of the absorption in the frequency domain,
$\alpha = \Delta\omega_{1/2}/c$

~130 Hz relative laser linewidth

Uncertainty of the fitted resonance frequency ~1 Hz

Uncertainty of the fitted width of the resonances ~0.04%

Absorption spectrum measured by observations of frequency for both the *x* and *y* axes.

et al., *Frequency-agile, rapid scanning spectroscopy: absorption sensitivity 0^{-12} cm^{-1} Hz$^{-1/2}$ with a tunable diode laser*, Appl. Phys. B **114**, 489-495 (2014)

et al., *Cavity mode-width spectroscopy with widely le ultra narrow laser*, Opt. Expr. **21**, 29744-29754 (2013)

One-dimensional frequency-based spectroscopy

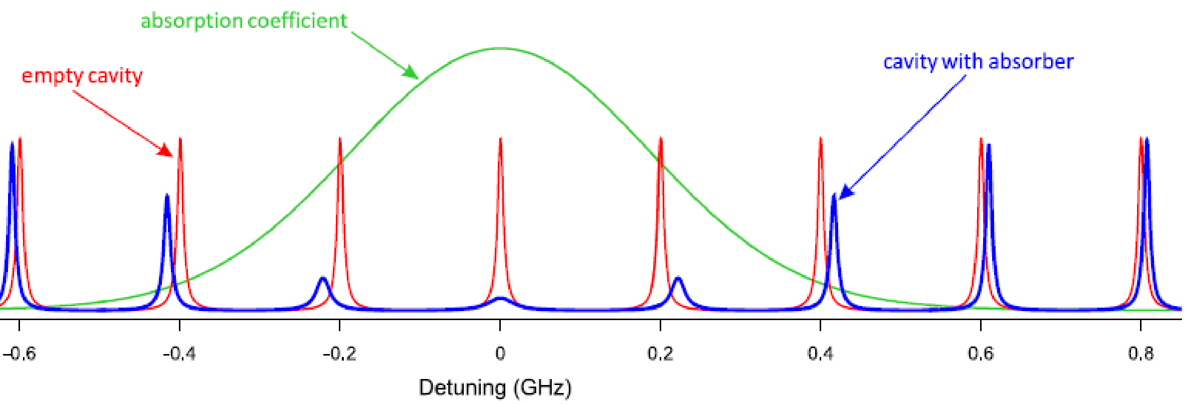

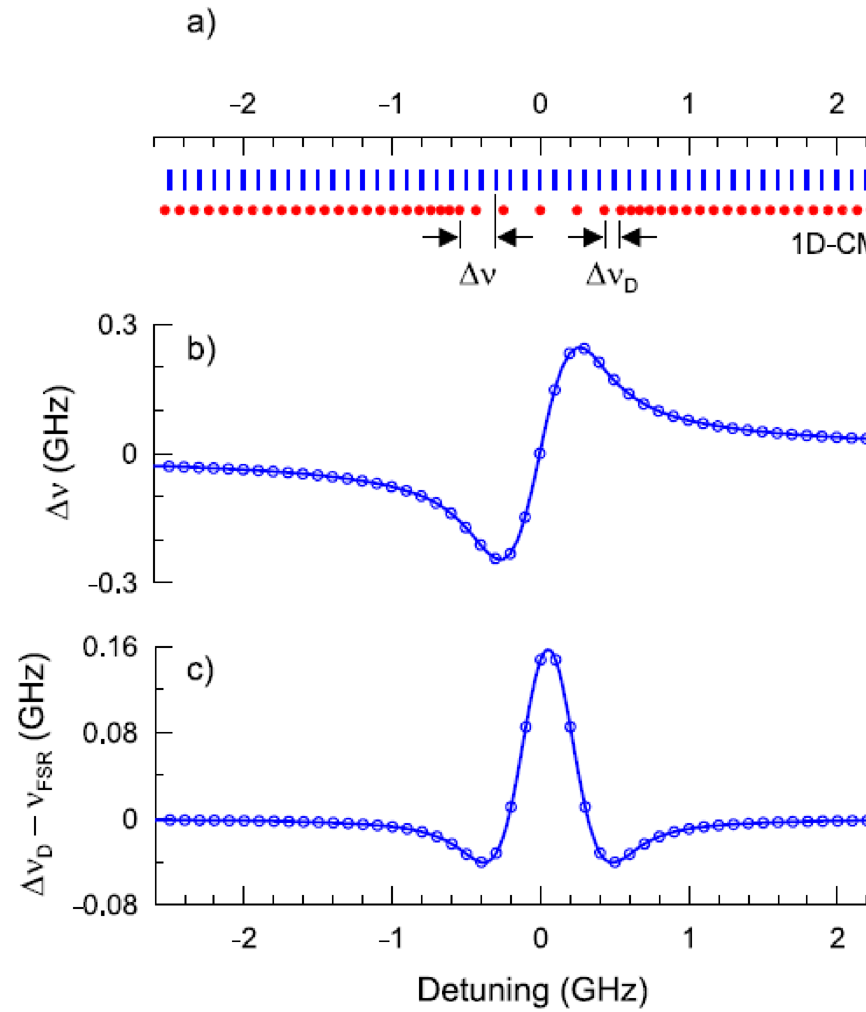

ption spectra (both *x* and *y* axes) obtained exclusively ns of frequency measurements

e potential for quantifying systematic uncertainty by rison to standard CRDS and mode-width measurements

al. Opt. Expr. **23**, 14472 (2015)

Thanks to

R.D. van Zee, D.A. Long, A.J. Fleisher,
Z. D. Reed, K.O. Douglass,
S.E. Maxwell, R.D van Zee, D.F. Plusquellic

Guest Researchers

K. Bielska,[*] H. Lin, M. Ghysels, G.W. Truong, V. Sironneau,
S. Wojtewicz,[*] A. Cygan[*]

[*]University of Nicolaus Copernicus, Torun, Poland
D. Lisak, R. Ciuryło

Funding: NIST Greenhouse Gas Measurements and Climate Research Program
NASA OCO- Science Team